Complete mitochondrial genome sequence of *Labriocimbex sinicus*, a new genus and new species of Cimbicidae (Hymenoptera) from China (#34672)

First revision

Guidance from your Editor

Please submit by **28 May 2019** for the benefit of the authors (and your $200 publishing discount).

Structure and Criteria
Please read the 'Structure and Criteria' page for general guidance.

Custom checks
Make sure you include the custom checks shown below, in your review.

Author notes
Have you read the author notes on the guidance page?

Raw data check
Review the raw data. Download from the location described by the author.

Image check
Check that figures and images have not been inappropriately manipulated.

Privacy reminder: If uploading an annotated PDF, remove identifiable information to remain anonymous.

Files
Download and review all files from the materials page.

1 Tracked changes manuscript(s)
1 Rebuttal letter(s)
13 Figure file(s)
5 Table file(s)
2 Other file(s)

Custom checks

DNA data checks

- Have you checked the authors data deposition statement?
- Can you access the deposited data?
- Has the data been deposited correctly?
- Is the deposition information noted in the manuscript?

New species checks

- Have you checked our new species policies?
- Do you agree that it is a new species?

Is it correctly described e.g. meets ICZN standard?

Structure and Criteria

2

Structure your review

The review form is divided into 5 sections. Please consider these when composing your review:

1. **BASIC REPORTING**
2. **EXPERIMENTAL DESIGN**
3. **VALIDITY OF THE FINDINGS**
4. General comments
5. Confidential notes to the editor

You can also annotate this PDF and upload it as part of your review

When ready submit online.

Editorial Criteria

Use these criteria points to structure your review. The full detailed editorial criteria is on your guidance page.

BASIC REPORTING

- Clear, unambiguous, professional English language used throughout.
- Intro & background to show context. Literature well referenced & relevant.
- Structure conforms to PeerJ standards, discipline norm, or improved for clarity.
- Figures are relevant, high quality, well labelled & described.
- Raw data supplied (see PeerJ policy).

EXPERIMENTAL DESIGN

- Original primary research within Scope of the journal.
- Research question well defined, relevant & meaningful. It is stated how the research fills an identified knowledge gap.
- Rigorous investigation performed to a high technical & ethical standard.
- Methods described with sufficient detail & information to replicate.

VALIDITY OF THE FINDINGS

- Impact and novelty not assessed. Negative/inconclusive results accepted. *Meaningful* replication encouraged where rationale & benefit to literature is clearly stated.
- All underlying data have been provided; they are robust, statistically sound, & controlled.
- Speculation is welcome, but should be identified as such.
- Conclusions are well stated, linked to original research question & limited to supporting results.

Standout reviewing tips

The best reviewers use these techniques

Tip	*Example*
Support criticisms with evidence from the text or from other sources	*Smith et al (J of Methodology, 2005, V3, pp 123) have shown that the analysis you use in Lines 241-250 is not the most appropriate for this situation. Please explain why you used this method.*
Give specific suggestions on how to improve the manuscript	*Your introduction needs more detail. I suggest that you improve the description at lines 57- 86 to provide more justification for your study (specifically, you should expand upon the knowledge gap being filled).*
Comment on language and grammar issues	*The English language should be improved to ensure that an international audience can clearly understand your text. Some examples where the language could be improved include lines 23, 77, 121, 128 – the current phrasing makes comprehension difficult.*
Organize by importance of the issues, and number your points	*1. Your most important issue* *2. The next most important item* *3. …* *4. The least important points*
Please provide constructive criticism, and avoid personal opinions	*I thank you for providing the raw data, however your supplemental files need more descriptive metadata identifiers to be useful to future readers. Although your results are compelling, the data analysis should be improved in the following ways: AA, BB, CC*
Comment on strengths (as well as weaknesses) of the manuscript	*I commend the authors for their extensive data set, compiled over many years of detailed fieldwork. In addition, the manuscript is clearly written in professional, unambiguous language. If there is a weakness, it is in the statistical analysis (as I have noted above) which should be improved upon before Acceptance.*

Complete mitochondrial genome sequence of *Labriocimbex sinicus*, a new genus and new species of Cimbicidae (Hymenoptera) from China

Yuchen Yan [1], **Gengyun Niu** [2], **Yaoyao Zhang** [1], **Qianying Ren** [1], **Shiyu Du** [1], **Bocheng Lan** [1], **Meicai Wei** [Corresp. 2]

[1] Lab of Insect Systematics and Evolutionary Biology, Key Laboratory of Cultivation and Protection for Non-Wood Forest Trees, Central South University of Forestry and Technology, Changsha, Hunan, China

[2] Jiangxi Normal University, Nanchang, Jiangxi, China

Corresponding Author: Meicai Wei
Email address: weim@jxnu.edu.cn

Labriocimbex sinicus Yan & Wei gen. et sp. nov. of Cimbicidae is described. Its mitochondrial genome is also reported. The new genus is similar to *Pseudoclavellaria* Schultz and *Trichiosoma* Leach. A key to extant Holarctic genera of Cimbicidae is provided. To identify the phylogentic placement of Cimbicidae, the mitochondrial genome of *L. sinicus* was annotated and characterized using high-throughput sequencing data. The complete mitochondrial genome of *L. sinicus* was obtained with a length of 15,405 bp (GenBank: MH136623 ; SRA: SRR8270383) and a typical set of 37 genes (22tRNAs, 13 PCGs, and two rRNAs). The results demonstrated that all PCGs were initiated by ATN codon, and ended with TAA or T stop codons. The study reveals that all tRNA genes have a typical clover-leaf secondary structure, except for *trnS1*. Remarkably, the secondary structures of the *rrnS* and *rrnL* of *L. sinicus* were much different from those of *Corynis lateralis*. Phylogenetic analyses verified the monophyly and positions of the three Cimbicidae species within the superfamily Tenthredinoidea and demonstrated a relationship as (Tenthredinidae + Cimbicidae) + (Argidae + Pergidae) with strong nodal supports. Furthermore, we found that a phylogenetic tree based on two methods shows that *L. sinicus* is the sister group of *Trichiosoma anthracinum* with high support values.

Complete mitochondrial genome sequence of *Labriocimbex sinicus*, a new genus and new species of Cimbicidae (Hymenoptera) from China

Yuchen Yan[1], Gengyun Niu[2], Yaoyao Zhang[1], Qianying Ren[1], Shiyu Du[1], Bocheng Lan[1], Meicai Wei[2]

[1]Lab of Insect Systematics and Evolutionary Biology; Key Laboratory of Cultivation and Protection for Non-Wood Forest Trees, Central South University of Forestry and Technology, Changsha, 410018, China.
[2] Jiangxi Normal University, Nanchang, Jiangxi, China

Corresponding Author:
Meicai Wei[2]
99 Ziyang Road, Nanchang, Jiangxi 330022, China
Email address: Email address: weim@jxnu.edu.cn

Abstract:

Labriocimbex sinicus Yan & Wei gen. et sp. nov. of Cimbicidae is described. Its mitochondrial genome is also reported. The new genus is similar to *Pseudoclavellaria* Schultz and *Trichiosoma* Leach. A key to extant Holarctic genera of Cimbicidae is provided. To identify the phylogentic placement of Cimbicidae, the mitochondrial genome of *L. sinicus* was annotated and characterized using high-throughput sequencing data. The complete mitochondrial genome of *L. sinicus* was obtained with a length of 15,405 bp (GenBank: MH136623; SRA: SRR8270383) and a typical set of 37 genes (22tRNAs, 13 PCGs, and two rRNAs). The results demonstrated that all PCGs were initiated by ATN codon, and ended with TAA or T stop codons. The study reveals that all tRNA genes have a typical clover-leaf secondary structure, except for *trnS1*. Remarkably, the secondary structures of the *rrnS* and *rrnL* of *L. sinicus* were much different from those of *Corynis lateralis*. Phylogenetic analyses verified the monophyly and positions of the three Cimbicidae species within the superfamily Tenthredinoidea and demonstrated a relationship as (Tenthredinidae + Cimbicidae) + (Argidae + Pergidae) with strong nodal support~~s~~. Furthermore, we found that a phylogenetic tree based on two methods shows that *L. sinicus* is the sister group of *Trichiosoma anthracinum* with high support values.

INTRODUCTION

Hymenoptera is one of the largest insect order including more than 153,000 species which possess very diverse life strategies (Peters *et al*., 2017). Currently, complete or nearly complete mitochondrial genomes have been reported for 199 hymenopteran species (NCBI, January 2019). The Cimbicidae is a small family of the superfamily Tenthredinoidea from the phytophagous ~~suborder~~ Symphyta ~~(Hymenoptera)~~, with about 197 valid species and 26 genera around the world. Within China, 63 species and 13 genera have already been recorded (Taeger *et al*., 2010; Yan and Wei, 2010; Blank *et al*., 2012; Yan and Wei, 2013; Yan *et al*., 2014; Yan and Wei, 2016; Yan *et al*., 2018). The monophyly of Tenthredinoidea is supported by both morphological (Wei and Nie, 1997) and molecular data (Malm and Nyman, 2015) as well as ~~both~~ combined (Ronquist *et al*., 2012; Sharkey *et al*. 2012; Klopfstein *et al*., 2013). However, the relationships among core tenthredinoids are unclear. Cimbicidae was inferred as the sister to Argidae + Pergidae proposed by morphological analyses (Wei and Nie, 1997; Vilhelmsen, 2001; 2015; 2018). The disaccord with several recent studies may be caused by the limited dataset of Cimbicidae, by molecular or combined analyses, which have placed Cimbicidae as sister to Diprionidae (Schulmeister, 2003; Schmidt and Walter, 2014; Isaka and Sato, 2015; Malm and Nyman, 2015) or a clade including Diprionidae form a monophylum as sister to the remaining tenthredinoids (Heraty *et al.*, 2011; Ronquist *et al.*, 2012; Klopfstein *et al.*, 2013).The monophyly of Cimbicidae has never been contested and not comprehensively tested until Vilhelmsen (2019). Adult Cimbicidae are primarily characterized by their clubbed antennae, one or more of the apical antennomeres being expanded. They vary in size from small (6mm) to very large insects (30mm), making them the largest true sawflies known (Vilhelmsen, 2019). Some of the species are economically important pests causing serious defoliation of woody plants such as

elm (*Ulmus*, Ulmaceae), willow (*Salix*, Salicaceae), honeysuckle (*Lonicera*, Caprifoliaceae) and cherry (*Prunus*, Rosaceae) (Gauld and Bolton 1988). Malaise (1934) established the classification of Cimbicidae: subfamily, tribe, subtribe and genus. Benson (1938) carried out a comprehensive study of sawflies, especially the members of Cimbicidae, which was further determined by the classification status of Cimbicidae. It included four subfamilies: Abiinae, Cimbicinae, Pachylostictinae and Corynidinae. The Cimbicinae is the most diverse subfamily and was best-supported monophyletic clade in the recent analysis of Cimbicidae (Vilhelmsen, 2019) but it is not supported as a monophyly group in cladistic analyses with sufficient representation of cimbicid taxa of China (Deng, unpublished). The Cimbicinae was divided into Cimbicini and Trichiosomini (Abe and Smith, 1991). The monophyly of Cimbicini was not supported by a following cladistic analyses with sufficient representation of cimbicid taxa of China (Deng, unpublished) and a cladistic analyses with most representatives of cimbicid taxa of world (Vilhelmsen, 2019). The monophyly of Trichiosomini was supported by a cladistic analyses with sufficient representation of cimbicid taxa of China (Deng, unpublished).

The new genus is closely similar to *Pseudoclavellaria* Schultz and *Trichiosoma* Leach by some morphological characters. Vilhelmsen (2019) sustained *Labriocimbex* placed as a grade basal to Cimbicinae, it was usually placed as the sister to *Cimbex* + *Odontocimbex* in the all strict consensus trees.

So far, mitochondrial genome of two species, *Trichiosoma anthracinum* (KT921411) and *Corynis lateralis* (KY063728) have been reported for the family (Song *et al*. 2016; Doğan and Korkmaz, 2017). Here, we reported one complete mitochondrial genome of *Labriocimbex sinicus*. We also compared it with the previously reported mitochondrial genomes of *T. anthracinum* and *C. lateralis* for better understanding of the mitochondrial genome characteristics of the Cimbicidae. Finally, we have performed phylogenetic analyses to verify the phylogenetic position of *Labriocimbex* using a mitochondrial genome dataset of 36 species from Hymenoptera (34 species of Symphyta and two species of Apocrita) with four non-hymenopteran outgroups (Table 1).

MATERIALS & METHODS

Description of new species

Specimens were examined with a Leica S8APO dissection microscope. Adult images were taken with a Nikon D700 digital camera and a series of images edited using Helicon Focus (HeliconSoft), while detailed images were taken with Leica Z16 APO/DFC550. A cylinder of semitransparent plastic was placed around the specimen to disperse the light, that methods follows Vilhelmsen (2019). The specimen must be sufficiently relaxed in a moist chamber before dissection. Dissected ovipositor valves, gonoforcep and penis valves were permanently mounted on slides in gum Arabic and images produced and composited automatically with a Nikon Ci-L/DS-Fi3. We used Adobe Photoshop CS 6.0 for further image processing. The terminology of sawfly genitalia follows Ross (1945), and that of general morphology follows Viitasaari (2002). For a few terms (e.g. middle fovea and lateral fovea), we followed Takeuchi (1952).

Abbreviations used were: OOL = distance between the eye and outer edge of lateral ocelli; POL = distance between the mesal edges of the lateral ocelli; OCL = distance between a lateral ocellus and the occipital carina or hind margin of the head.

The holotype and some paratypes of the new species are deposited in the Asian Sawfly Collection, Nanchang, China (ASCN). The most remaining paratypes are deposited in the Insect Collection of Central South University of Forestry and Technology, Changsha, Hunan, China (CSCS). A few paratypes are kept in Lishui Academy of Forestry (LSAF).

The electronic version of this article in Portable Document Format (PDF) will represent a published work according to the International Commission on Zoological Nomenclature (ICZN), and hence the new names contained in the electronic version are effectively published under that Code from the electronic edition alone. This published work and the nomenclatural acts it contains have been registered in ZooBank, the online registration system for the ICZN. The ZooBank LSIDs (Life Science Identifiers) can be resolved and the associated information viewed through any standard web browser by appending the LSID to the prefix http://zoobank.org/. The LSID for this publication is: urn: lsid: zoobank.org: pub: EE7F5193-78B2-42CE-87C1-B3FE947CB70F. The online version of this work is archived and available from the following digital repositories: PeerJ, PubMed Central and CLOCKSS.

DNA library construction and sequencing

Total DNA was extracted from *L. sinicus* using an E.Z.N.A. ® Tissue DNA Kit (Omega, Norcross, GA) and was stored at −20°C, in accordance with the manufacturer's instructions. Sequencing libraries with approximately 250-bp insertions were constructed using a NEXT flex™ Rapid DNA-Seq Kit (Illumina, San Diego, CA) in accordance with the manufacturer's protocol. Each library was sequenced using an Illumina Hiseq 4000 to generate 150-bp paired end reads at BGI-Shenzhen, China. The sequencing reads have been deposited in NCBI SRA database under accession number: PRJNA507477.

Mitochondrial genome assembly

Next generation sequencing and bioinformatic analyses were performed by Shanghai Majorbio Bio-pharm Technology Co., Ltd. Reconstruction of the mitochondrial genome from Illumina reads were carried out using three different approaches to ensure the accuracy of the assemblies: SOAPdenovo v2.0 (Luo *et al.*, 2012), MITObim v1.8 (Hahn *et al.*, 2013) and NOVOPlasty v2.7.1 (Dierckxsens *et al.*, 2017). The assembled mitochondrial fragments were identified using BlastX and *T. anthracinum* (NC029733) mitochondrial genes as queries. Prediction and annotation of protein-coding, tRNA and rRNA genes were performed using DOGMA (http://dogma.ccbb.utexas.edu/) or MITOS (http://mitos.bioinf.uni-leipzig.de/index.py) with annotation from a reference mitochondrial genome. Queries were then corrected manually.

Mitochondrial genome annotation and secondary structure prediction

All RNA genes were identified by employing the online MITOS tool (http://mitos.bioinf.uni-leipzig.de/index.py) (Bernt *et al.*, 2013) with the invertebrate mitochondrial genetic code. The initiation and termination codons of PCGs were determined using Geneious v11.0.3

(http://www.geneious.com) with reference sequences from other symphytan species with subsequent manual adjustment. The A + T content of nucleotide sequences and relative synonymous codon usage (RSCU) were calculated using MEGA v7.0 (Kumar *et al.*, 2016). Strand asymmetry was calculated using the formulae (Perna and Kocher, 1995): GC–skew = (G – C) / (G + C) and AT–skew = (A – T) / (A + T), for the strand encoding the majority of the PCGs.

The secondary structures of the *rrnS* and *rrnL* were partitioned into four areas and six areas, respectively. The secondary structures of rRNAs were inferred using alignment to models predicted for *T. anthracinum*. First, the primary sequence and the secondary structure of this species were aligned in MARNA (Siebert and Backofen, 2005) to identify a consensus sequence as well as a consensus structure in the output files. Secondly, the secondary structures of the *rrnS* and *rrnL* in *L. sinicus* were predicted by specific structure models in SSU-ALIGN (Nawrocki, 2009). Finally, the structures were artificially transformed to their relative secondary structure with micro changes.

The predicted secondary structures of RNAs were drawn using VARNA v3-93 (Darty *et al.*, 2009) and RNAviz 2.0.3 (De Rijk *et al.*, 2003). Helix numbering was performed following the *Apis mellifera* rRNA secondary structure (Gillespie, Johnston, Cannone, & Gutell, 2006) including minor modifications.

Phylogenetic analysis

We used the Maximum Likelihood (ML) and Bayesian Inference (BI) methods to construct phylogenetic trees of selected species, using 13 PCGs and two rRNAs (Table 1). The mitochondrial genome sequences of selected species were downloaded from GenBank. A total of 13 PCGs were aligned by MUSCLE in MEGA v7.0 individually, and two rRNAs were aligned by MAFFT (https://www.ebi.ac.uk/Tools/msa/mafft/) (Katoh & Standley, 2013). Then, the aligned nucleotide sequences of PCGs and rRNAs were concatenated using SequenceMatrix v1.7.8 (Vaidya *et al.*, 2011) and partitioned into several data blocks.

The partitioned data block file was used to infer both partition schemes and substitution models in PartitionFinder v1.1.1 (Lanfear *et al.*, 2012), with “unlinked” branch lengths under the “greedy” search algorithm. The standard partitioning schemes “bic” and “aicc” were selected for BI and ML analyses, respectively. BI analyses were conducted with the GTR+I+G model and HKY+G model using MrBayes v3.2.2 (Ronquist *et al.*, 2012). Four simultaneous Markov chains (three cold, one heated) were run for five million generations in two independent runs, with sampling every 100 generations and the first 25% of generations were discarded as burn-in.

The best partitioning scheme, such as: GTR+I+G, GTR+G and HKY+G for 13 PCGs were chosen (Table 2). The best-fit model of nucleotide substitution and phylogenetic construction based on ML was created using the IQ-TREE web server (http://iqtree.cibiv.univie.ac.at/). The previous data block file was used as well as the original parameters. In addition, 0.1 was employed as the disturbance intensity and 1000 as the IQ-TREE stopping rule. All related files have been uploaded to Figshare (https://figshare.com/s/b7e5b401b4881328c3b1).

RESULTS AND DISCUSSION

Description

***Labriocimbex* Yan & Wei, gen. nov.**

urn: lsid: zoobank. org: act: 29EB6C0E-881D-46E2-AEF0-3BDF5992EC37

Type species: *Labriocimbex sinicus* Yan & Wei, sp. nov.

Description. Body middle to large-sized; black, without metallic luster (Figure 1); head and thorax with dense and long yellowish brown hairs; clypeus distinctly broader than distance between lower margin of eyes, anterior margin with arcuate notch, furrow between clypeus and supraclypeal area deep (Figure 2A); base of labrum much broader than apex, lateral margin of labrum distinctly narrowed upward (Figure 2A); mandibles elongate, with three teeth in total, basal one truncate at apex (Figures 3A, 3B); maxillary palp with 6 palpomeres, apex 1–2 combined distinctly shorter than palpomere 4; labial palp with 4 palpomeres, short (Figure 2G); malar space 2.3 times the diameter of lateral ocellus, about as long as scape and pedicel combined; eyes moderately large, inner margins parallel, distance between eyes slightly longer than longest axis of eye (Figures 2A, 2B); lateral part of head distinctly dilated behind eyes in lateral view (Figure 2B) and dorsal view (Figure 2D); postocellar area with median and lateral furrows distinct, frontal carina indistinct (Figure 2D). Antennae longer than breadth of head, club of antennae strongly enlarged with obscure annular suture, with 5 antennomeres before club, antennomere 3 slender and distinctly longer than antennomeres 4 and 5 combined (Figure 2H). Propleuron and sternum merged; median suture of mesonotum shallow, notaulus distinct; mesoscutellum flat, anterior margin subtruncate, posterior margin roundly triangular (Figure 2E); distance between inner margin of cenchri 3.3 times the longest axis of a cenchrus, distance between outer margin of cenchri longer than breadth of mesoscutellum (Figure 2E). Coxae and femur of leg with long hairs; ventral side of middle and hind femur without tooth near apex (Figures 2F, 3C), hind coxae close to each other; inner spur of hind tibia as long as apical breadth of tibia, apex blunt and membranous (Figure 3J), about 0.4 times length of metabasitarsus; metabasitarsus slightly shorter than tarsomeres 2 and 3 combined, base of hind tibia narrower than apex (Figure 2F); 1st and 2nd tarsal pulvilli long, nearly contiguous (Figure 2F); claw simple, roundly bent (Figure 3K). Fore wing with crossvein 2r present, base of vein Rs absent (Figure 1A); vein 2r-m and 2m-cu almost interstitial, pterostigma long and narrow; anal cell strongly narrowed in basal 1/3 with a short anal crossvein, apical anal cell about 2 times the length of basal anal cell; cell Rs and M closed in hind wing, apex of anal cell quadrate, petiole of anal cell longer than length of vein cu-a, jugum region only with 1 longitudinal vein, without crossvein (Figure 1A). Sternites and basal abdominal terga with long hairs, posterior margin of abdominal tergum 1 shallowly incised, without middle carina and lateral carina (Figures 2E, 2F). Genital plate of female developed with wide incision and arcuate in middle (Figure 3L); apical ovipositor sheath short and roundish in lateral view (Figure 3D), tapering toward apes in dorsal view (Figure 3F); apex of lancet and lance curved upwards (Figures 3M, 3N), each annulus with

1 pore, serrulae sub-truncate at apex, lateral teeth sharp (Figure 3G). Each sternite of male incised in middle, both sides roundish (Figure 3E); penis valve broad, with apical lobe bulge, ventral hook small, lateral ridge distinct (Figure 3H); harpe small, longer than broad (Figure 3I).

Etymology. The generic name is composed of "*labrio-*" and "*-cimbex*", emphasizing the shape of labrum differs from other genera of the family. Gender masculine.

Distribution. China.

Host plant: *Prunus pseudocerasus* of Rosaceae (Female adult were observed laying eggs on it).

Remarks.

The name *Labriocimbex* was mentioned in two papers before (Li & Wu, 2010; Vilhelmsen, 2019). The name was a nomina nudum and not accompanied by a proper description and ~~the~~ type designation. ~~But~~ the name was really proposed by the senior author of this paper (MW) for the genus hear described as new to science. So the name was still used here.

This new genus is similar to *Pseudoclavellaria* Schultz and *Trichiosoma* Leach. It differs from *Pseudoclavellaria* by having the clypeus and labrum black; the base of labrum much wider than its apex and the basal breadth about half the breadth of clypeus; antennae with 5 antennomeres before the club; the anal cell strongly narrowed in basal 1/3 with a short crossvein and apical anal cell about 2 times the length of basal anal cell, the vein 2r-m and 2m-cu in fore wing almost interstitial. It differs from *Trichiosoma* by the ventral side of the hind femur without a subapical dent; the 1st and 2nd tarsal pulvilli in the male very long and nearly contacting to each other, and the different pattern of the male genitalia.

Trichiosomini includes 3 genera: *Pseudoclavellaria*, *Pseudoclavellaria* and *Leptocimbex* (Abe & Smith, 1991; Deng, unpublished). Most of the characteristics of the new genus suggest placing it in the tribe Trichiosomini. The most important characteristics include: the labrum large with the basal breadth about half the breadth of clypeus, the jugum region in hind wing without crossvein, the clypeus very short and much broader than lower distance between eyes and not merging with supraclypeal area. See the key below for the relationship of the new genus and other genera of the family.

Key to extant Holarctic genera of Cimbicidae

1 Anal cell of fore wing divided into two by a long medial constriction; clypeus not enlarged, distinctly narrower than distance between lower corners of eyes, or antennae with 5 antennomeres and nearly as long as head breadth; inner margins of eyes strongly convergent or strongly divergent downward ~~mandibles and hind legs in males not excessively enlarged compared to their females~~.....2

-- Anal cell of fore wing divided into two near the middle by a straight vein or seldom a punctiform petiole; clypeus distinctly broader than distance between lower corners of eyes; antennae at least with 6 ~~clear~~ antennomeres (except for *Pseudoclavellaria*) and distinctly longer than head breadth; inner margin of eyes subparallel or slightly convergent downward; ~~mandibles and hind legs in males normal or excessively enlarged compared to their females~~. **Cimbicinae**..... 6

2 Inner margins of eyes strongly convergent downward; distance between antennal toruli about 2 times as long as breadth of clypeus, clypeus not separated from supraclypeal area by a distinct transversal furrow; anterior tentorial small and shallow; head narrowed behind eyes in dorsal view, POL longer than OCL; hind orbit with distinct occipital carina; mesonotum with sulcus between mesoscutal lateral lobe and middle lobe almost obsolete; hind coxae separated, apex of tibial spur acute and sclerotinous. **Corynidinae**.....***Corynis*** Thunberg

-- Inner margins of eyes strongly divergent downward; distance between antennal toruli about as long as breadth of clypeus, clypeus separated from supraclypeal area by a distinct transversal furrow; anterior tentorial large and deep; head enlarged behind eyes in dorsal view, POL much shorter than OCL; hind orbit round, without occipital carina; mesonotum with sulcus between mesoscutal lateral lobe and middle lobe deep; hind coxae contiguous, apex of tibial spur blunt and membranous **Abiinae**.....3

3 Anterior margin of clypeus distinctly incised; body without metallic luster or with weak metallic luster.....4

-- Anterior margin of clypeus truncate; body usually with distinct metallic luster.....5

4 Claw bifurcate, inner tooth large; dorsal margins of eyes almost contact in male, distance narrower than basal breadth of flagellum.....***Orientabia*** Malaise

-- Claw with a small inner tooth at about middle; distance between dorsal margins of eyes in male broader than basal breadth of flagellum.....***Allabia*** Semenov & Gussakovskij

5 Claw simple; head and thorax with dense long hairs.....***Zaraea*** Leach

-- Claw bifurcate, inner tooth large; long hairs on head and thorax sparse or absent.....***Abia*** Leach

6 Labrum small, clearly narrower than 1/4 breadth of clypeus; ~~jugum region in hind wing with or without crossvein~~; clypeus narrower than lower distance between eyes, or clypeus triangularly convex and merging with supraclypeal area.....7

-- Labrum large, not narrower than 1/3 breadth of clypeus; ~~jugum region in hind wing without crossvein~~; clypeus very short and much broader than lower distance between eyes, not merging with supraclypeal area.....11

7 Jugum region in hind wing without crossvein; ventral side of middle and hind femora with 1- 2 rows of dents, or anal cell in fore wing with a punctiform middle petiole, or head narrowed behind eyes in dorsal view.....8

-- Jugum region in hind wing with a crossvein; middle and hind femora without dent ventrally; anal cell of fore wing with a middle crossvein; head not narrowed behind eyes in dorsal view [malar space distinctly broader than diameter of median ocellus; posterior margin of abdominal tergum 1 strongly incised; clypeus triangularly convex and merging with supraclypeal area].....10

8 Outer side of middle and hind coxae with a large dent; ventral side of hind femur with 1-2 rows of dents; mandibles simple, without inner tooth; malar space very long, clearly longer than antennomere 4; antennae with 8–9 antennomeres [claw simple].....***Odontocimbex*** Malaise

-- Outer side of coxae without dent; ventral side of femora without 1-2 rows of dents; mandibles with distinct inner tooth; malar space short, at most as long as antennomere 1, much shorter than antennomere 4; antennae with 6–7 antennomeres.....9

9 Clypeus clearly narrower than shortest distance between eyes and separated from supraclypeal area with a shallow but distinct furrow; anal cell in fore wing with a short petiole at basal third; claw simple; tibial spur stout, much shorter than apical breadth of tibia, apex obtuse; head enlarged behind eyes in dorsal view.....***Praia*** Andre

-- Clypeus clearly broader than shortest distance between eyes and merging with supraclypeal area, furrow between them absent; anal cell in fore wing with a distinct crossvein at basal fourth; claw bifurcate; tibial spur slender, clearly longer than apical breadth of tibia, tapering toward apex; head narrowed behind eyes in dorsal view.....***Agenocimbex*** Rohwer

10 Clypeus and supraclypeal area entirely merging together and without depression between them; distance between antennal toruli and posterior margin of head clearly shorter than distance between toruli and anterior margin of clypeus; postocellar area much broader than long; distance between cenchri about 5 times as long as breadth of a cenchrus.....***Palaeocimbex*** Semenov

-- Clypeus and supraclypeal area not entirely merging together and with a shallow depression between them; distance between antennal toruli and posterior margin of head about as long as distance between toruli and anterior margin of clypeus; postocellar area about as long as broad; distance between cenchri about 2-3 times as long as breadth of a cenchrus.....***Cimbex*** Olivier

11 Ventral side of middle and hind femur with ~~1~~ distinct dent near apex [clypeus and labrum black; labrum narrowed toward base.....***Trichiosoma*** Leach

-- Ventral side of femur without dent.....12

12 Head and thorax with dense and long hairs; club of antennae not segmented; abdominal tergum 1 without lateral carina; tarsal pulvilli large, 1st and 2nd pulvilli nearly touching to each other, first pulvillus longer than 1/2 length of basitarsus; apical anal cell of forewing 1 to 2 times length of basal anal cell.....13

-- Head and thorax without dense and long hairs; club of antennae distinctly segmented; abdominal tergum 1 at least with distinct lateral carina at basal 1/2; tarsal pulvilli short and small, separated each other, distance between basal 2 pulvilli not shorter than length of a pulvillus, first pulvillus much shorter than half length of basitarsus; fore wing with apical anal cell about 3 times length of basal anal cell.....***Leptocimbex*** Semenov

13 Labrum broadened toward base and distinctly narrowed toward apex; antennae with 6 antennomeres; inner spur of hind tibia as long as apical breadth of tibia; abdominal terga with long hairs; fore wing with apical anal cell 2 times as long as basal anal cell, vein 2m-cu almost interstitial to vein 1r-m; clypeus and labrum black.....***Labriocimbex*** Yan and Wei, gen. nov.

-- Labrum clearly narrowed toward base and distinctly broadened toward apex; antennae with 5 antennomeres; inner spur of hind tibia clearly shorter than apical breadth of tibia; abdominal terga without long hairs; forewing with apical anal cell as long as basal anal cell, vein 2m-cu remote from vein 1r-m; clypeus and labrum white.....***Pseudoclavellaria*** Schulz

362 ***Labriocimbex sinicus* Yan & Wei sp. nov. (Figures 1-3)**
363 urn: lsid:zoobank.org:act:E1454ED2-5321-4D39-97C2-EC8957D034C1
364
365 **Female. (Holotype)** Body length 21 mm (Figure 1A). Black; apical 1/2 of mandible reddish
366 brown (Figures 3A, 3B); inner and ventral side of club of antennae largely brown, outer side dark
367 brown (Figure 2H); cenchri pale yellowish white; posterior half of mesepimeron, metapleuron
368 largely, metanotum except for a small macula behind cenchri and most of metapostnotum,
369 median triangular macula and narrow posterior margin of abdominal tergum 1 (Figure 2E)
370 yellowish white; apex of each tibia, tarsus and claw reddish brown, tarsal pulvillus grayish white
371 (Figure 2F). Wings brownish hyaline, stigma black, basal 3/5 of vein C in fore wing, basal 3/7 of
372 vein Sc+R and entire vein M+Cu pale yellow, vein A pale brown, other veins largely black, vein
373 J and basal parts of all other veins in hind wing pale yellow (Figure 1A). Hairs on face and gena
374 black at base and yellowish white at apex (Figure 2A); hairs on vertex of head and mesonotum
375 black (Figure 2D); hairs on pronotum and scutellum yellowish white largely except for black
376 basal 0.2; hairs on mesopleuron, coxae and femora yellowish brown largely with less than basal
377 0.3 black (Figures 2C, 2E, 2F); inner hairs of fore tibia reddish yellow; abdominal terga 1–2 and
378 posterior margins of terga 3–4 with yellowish white hairs; hairs on ventral side of terga and
379 sternites 1–3 black in basal 0.4 and reddish yellow in apical 0.6.
380 Body densely microsculptured, matt; lower margin of orbit, small fovea lateral to lateral ocellus,
381 apical half of mandible, narrow lateral side of mesoscutal lateral lobe, ventral part of trochanters
382 and of femora distinctly shiny, ventral half of mesepisternum feebly microsculptured mixed with
383 some minute punctures, shiny; venter of abdomen feebly shiny.
384 Apex of labrum thickened with middle notch (Figure 2A); median fovea round and deep, lateral
385 foveae obscure (Figure 2D); middle of frons concave, lateral furrow of frons shallow; postocellar
386 furrow distinct, interocellar furrow long and deep; postocellar area quadrate, middle furrow very
387 shallow, indistinct; lateral furrows shallow, weakly divergent backwards (Figure 2D). Long hairs
388 on gena clearly shorter than 1/3 head width in dorsal view. Club of antennae as long as length of
389 antennomeres 4 and 5 combined, with obscure annular suture (Figure 2H). Mesopleuron without
390 middle oblique ridge (Figure 2C); cenchrus 2.1 times broader than long, reniform (Figure 2E).
391 Coxae and femora with dense hairs longer than breadth of femora (Figure 2F); inner hairs of tibia
392 dense and short (Figure 2F). Vein 2r in fore wing joining cell 2Rs at basal 0.4; cu-a joining cell
393 1M close to vein 1M (Figure 1A). Abdominal terga 1–2 and posterior margin of terga 3–4 with
394 dense and long hairs, other terga with sparse and short hairs. Sternites and ventral side of
395 abdominal terga with spare and long hairs (Figure 2F). Ovipositor sheath 0.8 times as long as
396 metatarsomere 1 and 2 combined, apical margin roundish in lateral view (Figure 3D), acute at
397 apex in dorsal view (Figure 3F). Lancet with 45 serrulae (Figure 3N), middle serrulae as Figure
398 3G, annular spine bands narrow, membranous area between serrulae roundly protruding, middle
399 serrulae subtruncate at apex, with 5–6 proximal and 4–5 distal subbasal teeth (Figure 3G).
400 **Male**: Body length 21.5 mm (Figure 1B); body color and structure similar to female except for
401 following parts: labrum broad and large; anterior margin of clypeus arc-shape, without incision;

metathorax and abdominal tergum 1 entire black; subgenital plate slightly broader than long (Figure 3E), apical margin round; apex of each sternite with clear middle incision, both sides roundly arcuate. Penis valve shown in Figure 3H, gonoforcep shown in Figure 3I.

Holotype. Female (CSCS13010_Lab001). China: Hunan Province, Wugang County, Mt. Yun, Yunfengge alt. 1,380 m, 26°38.630' N, 110°37.299' E, April 13, 2013, Zejian Li leg.

Paratypes: 17 Females, 15 Males (CSCS13010_Lab002–033). Collecting information as the holotype. 18 Females, 10 Males (CSCS13015_Lab034–061), locality and collector as the holotype, April 15, 2013. 45 Females, 17 Males (CSCS13014_Lab062–123), locality and collecting time as the holotype, Liwei Qi, Biao Chu leg. 36 Females, 51 Males (CSCS11009_Lab124–210), China: Hunan Province, Wugang County, Mt. Yun, Shengli Temple, alt. 1,145 m, 26°38.859' N, 110°37.026' E, April 18-22, 2011, Zejian Li, Liwei Qi leg. 17 Females, 22 Males (CSCS05001_Lab211–249), China: Hunan Province, Wugang County, Mt. Yun, alt. 800-1,100 m, April 24-26, 2005, Meicai Wei, Shaobing Zhang, Wei Xiao leg. One Male (CSCS1999001_Lab250), China: Hunan Province, Wugang County, Mt. Yun, alt. 1,300 m, April 3, 1999, Wei Xiao leg. Two Females, six Males (LSAF18029_Lab251–258), China: Zhejiang Province, Lin'an City, Mt. Tianmu, alt.1,506, 30.349°N, 119.424°E, April 19, 2018, Zejian Li, Mengmeng Liu leg. One Females (LSAF17053_Lab259), locality and collector as the former, April 16, 2017. One Females, 26 males (LSAF17054_Lab259–285), locality as the former, April 17, 2017, Tingting Ji leg. Four Females, two Males (CSCS18006_Lab286–291), China: Hunan Province, Wugang County, Mt. Yun, alt. 1,124 m, 26°38.059' N, 110°37.017' E, April 03, 2018, Meicai Wei, Gengyun Niu, Hannan Wang leg. Seven Females, one Males (CSCS18007_Lab292–299), locality as the former, alt. 1,129 m, 26°39.003' N, 110°37.027' E, April 04, 2018, Meicai Wei, Hannan Wang leg.

Variation. Body length 18-24mm in female, 19-24mm in male; club of antennae color brown to pale yellowish brown; hairs color on pronotum and scutellum yellowish white to yellowish brown.

Distribution. China (Hunan, Zhejiang).

Etymology: The specific name of the new species refers to the distribution area, China.

Remarks.

Labriocimbex pilosus sp. nov. (Li & Wu, 2010) and *Labriocimbex sinicus* (Vilhelmsen, 2019) were two nomina nuda and have never been described before this paper. ~~But~~ the two manuscript names were really proposed by the senior author of this paper (MW) for the two undescribed species found in China. The former species represents only by a few specimens from different localities and so it is not described here.

Labriocimbex sinicus Yan & Wei, sp. nov. is similar to *L. zaraeoides* (Malaise, 1939) comb. nov. (Figure 4A), but differs from the latter in the following characters: the clypeal notch deep, depth about 1/2 length of clypeus; between the clypeus and supraclypeal area with a distinct transverse furrow; the long hairs on gena 3.5 times as long as diameter of lateral ocellus, longer than the shortest axis of an eye; the long hairs on mesopleuron about 4.5 times as long as diameter of lateral ocellus; the abdominal tergum 1 largely black.

Labriocimbex pilosus nomina nuda differs from *L. sinicus* in the following characters: the thorax with fine and dense hairs, the fine hairs of abdomen sparser than those of thorax, the hair density

of each abdominal tergum resembled; the malar space 1.3 times as long as diameter of the lateral ocellus; the postocellar area transverse, distinctly broader than long; the metanotum, the metapleuron and the abdominal tergum 1 entirely black, the abdominal sternites 3–7 largely yellow brown or pale brown; the distance between the inner margins of eyes distinctly shorter than the longest axis of eye; the body length 13mm (female). Specimen collection record: one female, China, Gansu Province, Mt. Xiaolong, Maiji forest farm, Sun hill; alt. 1,620, 34°25′11.0″N, 105°46′30.1″E, April 17, 2009, Wu XingYu leg.

***Labriocimbex zaraeoides* (Malaise, 1939) comb. nov**. (Figure 4)

Trichiosoma zaraeoides Malaise, 1939: 16–17.

Distribution. Northern Myanmar.

Remarks. This species is similar to *L. sinicus* Yan & Wei sp. nov., the majority of the characters place it in the new genus *Labriocimbex.* The most important of these characters are: the broadly emarginated clypeus, the triangular labrum (Figure 4C), the form of the antennae (antennae with 5 antennomeres before the rigid club; joints of the club very indistinct [sic!] Malaise, 1939); the slender hind legs (the coxae and femur of leg with long hairs; the ventral side of hind femur without a dent near apex; the base of hind tibia narrower than apex; the 1st and 2nd tarsal pulvilli long, Figure 4D) the venation (the anal crossvein punctiform and the anal cell strongly narrowed, Figure 4A); the color of body (the posterior half of mesepimeron, metapleuron, metanotum and abdominal tergum 1 yellowish white, Figures 4B, 4D and 4G). The characters that separate this species from all known *Trichiosoma* are the yellowish white color of the metanotum and the base of the abdomen, and the ventral side of the hind femur without a large dent near apex. *L. zaraeoides* differs from *L. sinicus* in the following characters: the clypeal notch shallow, depth about 1/4 length of clypeus; the transverse furrow between clypeus and supraclypeal area absent (Figure 4C); the long hairs on gena 2.5 times the diameter of lateral ocellus, shorter than the shortest axis of an eye (Figure 4E); the long hairs on mesopleuron about 3.5 times as long as diameter of the lateral ocellus (Figure 4B); the abdominal tergum1 largely yellow brown (Figure 4G).

General features of the *L. sinicus* mitochondrial genome

We sequenced the complete mitochondrial genome of *L. sinicus* (GenBank accession no. MH136623), a typical set of 37 genes, including 13 PCGs, 22 tRNAs and two rRNAs. Most of the genes were located on the J strand except for four PCGs, two rRNAs and seven tRNAs (Table 3).

A total of 14 pairs of genes were directly adjacent, without overlapping or intergenic nucleotides. The total length of the intergenic regions was 268 bp in 18 locations with a size ranging from 1 to 50 bp (Table 3). The longest was located between *trnH* and *ND4*, while the second longest was 45 bp located between *rrnS* and *trnM*. In comparison with the mitochondrial genome of *T. anthracinum* and *C. lateralis*, there were differences in the length of intergenic spacers and locations. The longest (414 bp) was located at the start of the mitochondrial genome before *trnY* in *T. anthracinum*. The longest length of the intergenic spacers was 345 bp located between the

ND6 and *CYTB* genes in *C. lateralis*. We found that homologous searches on the longest intergenic region of *L. sinicus* revealed substantial differences from any identified Symphyta sequence.

There were in total 32 overlapping nucleotides between neighboring genes in six locations, and the range of length of the overlapping sequence is from 3 to 14 bp: *trnM* and *trnQ*, *ATP8* and *ATP6*, *ND4* and *ND4L*, *trnN* and *trnS2*, and *ATP6* and *COIII*; and the longest was 14 bp between *ATP6* and *COIII* (Table 3). The common motifs such as: ATGATAA between *ATP8* and *ATP6*, and ATGTTAA between *ND4* and *ND4L*, which also exist in *T. anthracinum*, and are not found in *C. lateralis*, are common features of many other insect mitochondrial genomes (Song *et al*., 2016; Doğan and Korkmaz, 2017).

Protein-coding genes and codon usage

The mitochondrial genome of *L. sinicus* contains 13 PCGs, and its length is 12,456 bp, accounting for 80.86% of the total length (Table 4). All PCGs were initiated by ATN codons. All PCGs were ended with TAA as stop codon except for *ND5* which ended with T (Table 3).

The codon usage of *L. sinicus* also shows a significant bias towards A/T Leu, Ile, Phe and Ser, were found as the most frequently used amino acids. TTA-Leu showed the highest RSCU of 5.04 (Table 5). Comparisons of the RSCU with those of *C. lateralis* and *T. anthracinum* showed a similar pattern for codon usage bias and reflected a significant correlation between codon preference and nucleotide composition, that is similar to other symphytan species (Dowton *et al*., 2009; Wei *et al*., 2010; 2015; Korkmaz *et al*., 2015, 2016, 2017; Song *et al*., 2015, 2016; Niu *et al*., 2018; Du *et al*., 2018; Ma *et al*., 2019; Tang *et al*., 2019). Codons rich in C and G, CGC-Arg and CTC-Leu was absent, CGG-Arg, GGC-Gly, AGC-Ser, ACG-Thr, CTG-Leu, GTC-Val, GTG-Val and TGC-Cys, were used once, AGG-Ser, TCG-Ser, TCC-Ser, CCG-Pro and GCG-Ala were rarely used, which is similar to both cimbicid mitochondrial genomes (Table 5). The ratio can be calculated by rate of G + C rich codons (Pro, Ala, Arg, and Gly) and A + T rich codons (Phe, Ile, Met, Tyr, Asn, and Lys), and it is 0.28 in *L. sinicus*, which is similar to those of other symphytan species (0.28–0.31) (Korkmaz *et al*., 2015). The translation, initiation, and termination signals as well as the codon usage of the *L. sinicus* mitochondrial genome do not display any unusual characteristics (Table 5).

Gene rearrangement and nucleotide composition

The mitochondrial genome of symphytan species appears to be more conserved than that of Apocrita (Song et al., 2016; Wei et al., 2014). However, compared with the putative ancestral mitochondrial genome of insects, we detected several rearrangement events in three tRNA gene clusters in *L. sinicus* (Figure 5), The first rearrangement event is found in the clusters of *trnI-trnQ-trnM*, where *trnM* and *trnQ* was founding swapped positions, in addition, *trnM-trnQ* was translocated from the *trnI-trnQ-trnM* cluster to a downstream position of *rrnS*; which have not been reported for any symphytan mitogenome to date. The second event is corresponding to the remote inversion of *trnY* and the translocation of *trnC* from a location between *trnW* and *cox1* to upstream of *trnI*, which has great similarity to the gene order and rearrangement events observed in *T. anthracinum*. The arrangement of cluster of *trnW-trnC-trnY* appears to be mostly

conserved in almost all known symphytan mitogenomes, except for representative cimbicid species. The last event is only found in the TP cluster of *L. sinicus*, and here *trnT* is inverted. The gene order from *COI* to *rrnS* is conserved in all sequenced species of Cimbicidae.

Similar to previously reported symphytan mitochondrial genomes (Ma *et al*., 2019; Doğan and Korkmaz, 2017; Song *et al*., 2016), the nucleotide compositions of *L. sinicus* (43.5% A, 37.7% T, 7.7% G and 11.1% C) were biased towards A and T, with an average 81.2% A+T content; a stronger AT bias was found in the N strand (81.4% A+T content) than in the J strand (78.7%) (Table 4).

Further analysis of the PCGs indicated that the third codon position demonstrates the highest A + T content (93.5%), in agreement with symphytan mitochondrial genomes (Ma *et al*., 2019; Doğan and Korkmaz, 2017; Song *et al*., 2016). The gene with the highest A + T content was *ATP8* with 88.3% (Table 4). Here we observed that the AT-skew was slightly positive (0.0714), and the GC-skew was negative (−0.1809) when considering the whole genome (Table 4). This indicates that the occurrence of A is higher than that of T, and the occurrence of C is higher than that of G, which is a general phenomenon observed in all reported symphytan mitochondrial genomes, except for those of *Tremex columba* and *Xiphydria* sp. (Ma *et al*., 2019; Doğan and Korkmaz, 2017; Song *et al*., 2016; Wei *et al*., 2015; Castro and Dowton, 2005; Dowton *et al*., 2009). However, a deviation was found in the PCGs of *L. sinicus*, in terms of AT-skew (−0.1389) and GC-skew (0.0348), which also occurred in both *C. lateralis* and *T. anthracinum*. This deviation can exert influences on the selection forces acting on the PCG codon positions, in accordance with study by Korkmaz (2015).

Transfer RNA genes

In the mitochondrial genome of *L. sinicus* 15 tRNAs were encoded by the J strand, while the remaining tRNAs were encoded by the opposite N-strand. All tRNAs folded into a common clover-leaf structure, except *trns1*-AGN, where the dihydrouridine (DHU) arm was missing (Figure 6). The size of the tRNAs ranged from 64 bp (*trnG*) to 71 bp (*trnC, trnK*), and this usually depends on the length of the variable loop, TΨC loop and D-loops (Clary and Wolstenholme, 1985). The DHU arm was 3–4 bp, the AC arm was 4–5 bp, and the TΨC arm varied from 4–5 bp, while the amino acid acceptor (AA) stem and anticodon (AC) loops were conserved at 7 bp in all of the tRNA genes.

In the mitochondrial tRNA secondary structures, mismatches mainly occur in the DHU arm, AA arm and AC arm, and sometimes in the TΨC arm. A total of 16 unmatched base pairs were scattered among the following tRNA genes, including 12 G-U mismatched pairs occurring in *trnA*, *trnD*, *trnQ*, *trnG*, *trnH*, *trnL1*, *trnP*, *trnF*, and *trnY*, and four U-U mismatches occurring in *trnR*, *trnT* and *trnL1*. The number of mismatches were 24 (12 G–U pairs, five U–U pairs, three A–A pairs, two A–C pairs, one A–G pair and one C–U pair) in *C. lateralis* (Figure 7, adapted from Doğan and Korkmaz, 2017), and 18 (15 G–U pairs, two U–U pairs and 1 A–C pair) in *T. anthracinum* (Figure 6; adapted from Song *et al*., 2016), which is typical for Hymenoptera (Ma *et al*., 2019; Castro and Dowton, 2005; Dowton *et al*., 2009b). The phenomenon of aberrant mismatches, loops, or extremely short arms for tRNAs has been shown to be common in metazoan mitochondrial genomes (Wolstenholme, 1992).

In addition, there were some tRNA structural differences between *L. sinicus* and *T. anthracinum* (Figure 6). The identified anticodons were almost identical to those of the cimbicid species, with the exception of the anticodon of *trnS1* (*AGn*), which is UCU in *L. sinicus* and *T. anthracinum*, as well as this is true of all previously reported of Symphyta (Ma *et al*., 2019; Doğan and Korkmaz, 2017; Song *et al*., 2016; Castro and Dowton, 2005; Dowton *et al*., 2009b).

Ribosomal RNA genes

The *rrnL* gene of *L. sinicus* was 1,341 bp in length with an 84.2% A+T content, while *rrnS* was 791 bp in length with an 84.1% A+T content (Table 4). This was in a comparable range to homologous genes in *T. anthracinum* (1,351 bp; 800 bp) and *C. lateralis* (1,359 bp; 493 bp *rrnS* partial gene), and also identical to all reported hymenopteran species (Gillespie, 2006; Wei *et al*., 2010, Doğan and Korkmaz, 2017; Song *et al*., 2016; Korkmaz *et al*., 2015). Both genes were encoded on the N-strand (Table 3).

Similar to the known symphytan mitochondrial genomes, the *rrnL* gene is positioned between *trnL1* and *trnV* in three species of Cimbicidae (Figure 5). The predicted structure of *rrnL* in *L. sinicus* is consistent with the observed pattern in *C. lateralis* and *T. anthracinum*, whereby 45 helices belonging to five domains were identified in those species (Figures 8, 9). Domain III is absent as in other arthropods (Korkmaz *et al*., 2015), and domain II is variable in base composition, forming a long stem with a big loop structure in the area II terminal. Domains IV and V are more conserved within the Tenthredinidae than domains I, II and VI. Eight helices (H563, H579, H777, H822, H2023, H2043, H2455 and H2547) of *rrnL* are highly conserved. The H183, H991, H1057, H1196 and H2077 helices display helical length and loop size/structure variability within three cimbicid *rrnL* genes (Figures 8, 9).

The *rrnS* secondary structure of *L. sinicus* is between *trnV* and an AT-rich region, and contains four domains and 26 helices. Compared with *T. anthracinum,* it is significantly different in terms of base composition in domain II (Figure 10). Specifically, H47 is variable among the different hymenopteran species, having a large loop. The loop size is variable and determined by overall *rrnS* length, except for in the cephid species (Gillespie, 2006; Wei *et al*., 2010, Doğan and Korkmaz, 2017; Song *et al*., 2016; Korkmaz *et al*., 2015). The structures of domains I and II of *C. lateralis* are missing, so they cannot be compared with those of *L. sinicus*, but the structures are similar in domains III and IV (Figure 11). In *rrnS*, domain III and domain VI were more conserved within Tenthredinidae than domains I and II (Figures 10, 11).

Phylogenetic relationships

Phylogenetic relationships within the suborder Symphyta were reconstructed using both BI and ML analyses (Figures 12 and 13, respectively). The topologies of the two phylogenetic trees were almost identical, especially the clade consisting of (Tenthredinidae + Cimbicidae) + (Argidae + Pergidae), which was very stable with the highest nodal supports. The recovered trees supported a relationship consisting of Xyelidae + (Tenthredinoidea + ((Megalodontesidae + Pamphiliidae) + (Xiphydriidae + (Cephidae + (Orussidae + (Apocrita + Siricidae)))))) in the Hymenoptera. The main parts of the cladograms were also supported by both molecular (Malm and Nyman 2014; Peters *et al*., 2017) and morphological studies (Schulmeister *et al*., 2002,

Vilhelmsen, 2001; 2015), except for Siricidae being the sister group of Apocrita. Although, *Tremex columba* (MH422968) as sister to *Tremex columba* (AY206795) in the phylogenetic inference based on IV and V areas of *rrnL* (YY Zhang, 2019, unpublished data), suggests the former is valid. More mitogenomes should be involved to evaluate the correctness of these unusual sister groups.

Both trees indicate that *L. sinicus* is grouped with *T. anthracinum* and formed a sister group to *C. lateralis*. We demonstrated that mitochondrial genome sequences can be used to solve phylogenetic relationships at different taxonomic levels within Symphyta.

CONCLUSIONS

Labriocimbex gen. nov. was regarded similar between the genera *Trichiosoma* Leach and *Pseudoclavellaria* Schultz. Most of the characteristics of the new genus suggest placing it in the tribe Trichiosomini. The most important characteristics include: the labrum large with the basal breadth about half the breadth of clypeus, the jugum region in hind wing without crossvein, the clypeus very short and much broader than lower distance between eyes and not merging with supraclypeal area. Following characters help to distinguish this new genus and new species: the clypeus and labrum black; the clypeus broadly and shallowly emarginated; the labrum triangular and tapering toward apex, basal breadth about half the breadth of clypeus; the apical anal cell about 2 times as long as basal anal cell; antennae with an apical club unsegmented and with 5 antennomeres before the club; the hind femora close to each other and without ventral dent; the very large tarsal pulvilli; malar space 2.3 times the diameter of lateral ocellus; the inner margins of eyes parallel; head distinctly dilated behind eyes; the inner spur of hind tibia as long as apical breadth of tibia, apex blunt and membranous; the long and dense hairs covering head, thorax, base of abdomen and legs.

The complete mitochondrial genome of *L. sinicus* was obtained and was found to have a length of 15,405 bp and a typical set of 37 genes. The secondary structures of the 22 tRNAs and two rRNAs resemble those of Symphyta. In comparison with the structures of *T. anthracinum* and *C. lateralis*, some helices were highly variable in *rrnL* and *rrnS*. Phylogenetic reconstruction showed similarly high levels of support (100%) in both BI and ML analyses that the family Cimbicidae is a sister group of ((*L. sinicus* + *T. anthracinum*) + *C. lateralis*).

The same results were obtained using two different analytical methods, and our findings agree with traditional morphological classification and recent molecular studies. The tree topologies confirm the newly sequenced taxonomic positions of the Cimbicidae species within the superfamily Tenthredinoidea, and reveal a relationship of (Tenthredinidae + Cimbicidae) + (Argidae + Pergidae) in Symphyta with strong nodal supports.

ACKNOWLEDGMENTS

Thank Dr. Zejian Li of the Lishui Academy of Forestry, Zhejiang province, China, for collecting specimens from Mt. Tianmu. The members of Lab of Insect Systematics and Evolutionary

Biology (LISEB) from Central South University of Forestry and Technology are thanked for their contributions in laboratory work. We thank all the reviewers for their comments.

REFERENCES

Abe M, Smith DR. 1991. The genus-group names of Symphyta (Hymenoptera) and their type species. *Esakia* 31: 1–115.

Beard CB, Hamm DM, Collins FH. 1993. The mitochondrial genome of the mosquito *Anopheles gambiae*: DNA sequence, genome organization, and comparisons with mitochondrial sequences of other insects. *Insect Molecular Biology* 2(2): 103–124.

Benson RB. 1938. On the classification of Sawflies (Hymenoptera, Symphyta). *Transactions of the Entomological Society of London* 87: 353–384.

Bernt M, Donath A, Jühling F, Externbrink F, Florentz C, Fritzsch G, Pütz J, Middendorf M, Stadler PF. 2013. MITOS: improved de novo metazoan mitochondrial genome annotation. *Molecular Phylogenetics and Evolution* 69: 313–319.

Blank SM, Groll EK. Liston A, Prous M, Taeger A. 2012. ECatSym - Electronic World Catalog of Symphyta (Insecta, Hymenoptera). Program Version 4.0 Beta, Data Version 39. Digital Entomological Information, Müncheberg. URL http://sdei.senckenberg.de/ecatsym.

Castro LR, Dowton M. 2005. The position of the Hymenoptera within the Holometabola as inferred from the mitochondrial genome of *Perga condei* (Hymenoptera: Symphyta: Pergidae). *Molecular Phylogenetics and Evolution* 34(3): 469–479.

Dierckxsens N, Mardulyn P, Smits G. 2017. NOVOPlasty: de novo assembly of organelle genomes from whole genome data. *Nucleic Acids Research* 45: 18.

De Rijk P, Wuyts J, De Wachter R. 2003. RnaViz 2: an improved representation of RNA secondary structure. *Bioinformatics* (Oxford, England) 19: 299–300.

Darty K, Denise A, Ponty Y. 2009. VARNA: Interactive drawing and editing of the RNA secondary structure. *Bioinformatics* 25: 1974–1975.

Doğan Ö, Korkmaz EM. 2017. Nearly complete mitogenome of hairy sawfly, *Corynis lateralis* (Brullé, 1832) (Hymenoptera: Cimbicidae): rearrangements in the IQM and ARNS1EF gene clusters. *Genetica* 145: 341–350.

Dowton M, Cameron SL, Austin AD, Whiting MF. 2009. Phylogenetic approaches for the analysis of mitochondrial genome sequence data in the Hymenoptera – a lineage with both rapidly and slowly evolving mitochondrial genomes. *Molecular Phylogenetics and Evolution* 52: 512–519.

Du SY, Niu GY, Nyman T, Wei MC. 2018. Characterization of the mitochondrial genome of *Arge bella* Wei & Du sp. nov. (Hymenoptera: Argidae). *PeerJ* 6: e6131.

Foster PG, Jermiin LS, Hickey DA. 1997. Nucleotide Composition Bias Affects Amino Acid Content in Proteins Coded by Animal Mitochondria. *Journal of Molecular Evolution* 44: 282–288.

Gillespie JJ, Johnston JS, Cannone JJ, Gutell RR. 2006. Characteristics of the nuclear (18S, 5.8S, 28S and 5S) and mitochondrial (12S and 16S) rRNA genes of *Apis mellifera* (Insecta:

689 Hymenoptera): structure, organization, and retrotransposable elements. *Insect molecular*
690 *biology* 15: 657–686.
691 Gauld I, Bolton B.1988. The Hymenoptera. British Museum (Natural History). Oxford
692 University Press, Oxford.
693 Hahn C, Bachmann L, Chevreux B. 2013. Reconstructing mitochondrial genomes directly from
694 genomic next-generation sequencing reads – a baiting and iterative mapping approach. *Nucleic*
695 *Acids Research* 41: 129–129.
696 Heraty J, Ronquist F, Carpenter JM. Hawks D, Schulmeister S, Dowling AP, Murray D, Munro
697 J, Wheeler WC, Schiff N, Sharkey M. 2011. Evolution of the hymenopteran megaradiation.
698 *Molecular Phylogenetics and Evolution* 60: 73–88.
699 Hyde J, Cooper SJB, Munguia P, Humphreys WF, Austin AD. 2018. The first complete
700 mitochondrial genomes of subterranean dytiscid diving beetles (*Limbodessus and Paroster*)
701 from calcrete aquifers of Western Australia. *Australian Journal of Zoology* 65: 283–291.
702 Isaka Y, Sato, T. 2015. Was species diversification in Tenthredinoidea (Hymenoptera:
703 Symphyta) related to the origin and diversification of angiosperms? *The Canadian*
704 *Entomologist* 147: 443–458.
705 Korkmaz EM, Aydemir HB, Temel B, Budak M, Başıbüyük HH. 2017. Mitogenome evolution
706 in Cephini (Hymenoptera: Cephidae): Evidence for parallel adaptive evolution. *Biochemical*
707 *Systematics and Ecology* 71: 137–146.
708 Korkmaz EM, Budak M, Ördek MN, Başibüyük HH. 2016. The complete mitogenomes of
709 *Calameuta filiformis* (Eversmann, 1847) and Calameuta idolon (Rossi, 1794) (Hymenoptera:
710 Cephidae): The remarkable features of the elongated A+T rich region in Cephini. *Gene* 576:
711 404–411.
712 Korkmaz EM, Doğan Ö, Budak M, Başibüyük HH. 2015. Two nearly complete mitogenomes of
713 wheat stem borers, *Cephus pygmeus* (L.) and *Cephus sareptanus* Dovnar-Zapolskij
714 (Hymenoptera: Cephidae): An unusual elongation of *rrnS* gene. *Gene* 558: 254–264.
715 Korkmaz EM, Doğan Ö, Durel BS, Temel Altun B, Budak M, Başıbüyük HH. 2018.
716 Mitogenome organization and evolutionary history of the subfamily Cephinae (Hymenoptera:
717 Cephidae). *Systematic Entomology* 43(3): 606–618.
718 Kumar S, Stecher G, Tamura K. 2016. MEGA7: Molecular Evolutionary Genetics Analysis
719 version 7.0 for bigger datasets. *Molecular Biology and Evolution* 33: 1870.
720 Klopfstein S, Vilhelmsen L, Heraty JM, Sharkey M, Ronquist F. 2013. The Hymenopteran Tree
721 of Life: Evidence from Protein-Coding Genes and Objectively Aligned Ribosomal Data).
722 *PLoS ONE* 8(8): e69344.
723 Katoh K, Standley DM. 2013. MAFFT multiple sequence alignment software version 7:
724 improvements in performance and usability. *Molecular Biology and Evolution* 30: 772–80.
725 Lanfear R, Calcott B, Ho SYW, Guindon S. 2012. Partition Finder: Combined selection of
726 partitioning schemes and substitution models for phylogenetic analyses. *Molecular Biology*
727 *and Evolution* 29: 1695–1701.

Li YG, Wu XY. 2010. The Investigation and Taxonomical Research of the Sawflies Species from Gansu Province Ⅲ. A list of the genera and species (Hymenoptera: Cimbicidae). *Journal of Gansu Forestry Science and Technology* 35(1): 12–14.

Luo R, Liu B, Xie Y, Li Z, Huang W, Yuan J, He G, Chen Y, Qi P, Liu Y. 2012. SOAPdenovo2: an empirically improved memory-efficient short-read de novo assembler. *Giga science* 1: 18.

Malm T, Nyman T. 2015. Phylogeny of the symphytan grade of Hymenoptera: new pieces into the old jigsaw (fly) puzzle. *Cladistics* 31: 1–17.

Malaise R.1934. Schwedisch-chinesische wissenschaftliche Expedition nach den nordwestlichen Provinzen Chinas unter Leitung von Dr. Sven Hedin und Prof. Sü Ping-Chang. Insekten gesammelt vom schwedischen Arzt der Expedition Dr. David Hummel 1927–1930.

Malaise R. 1939. The Genus *Leptocimbex* Sem., and some other Cimbicidae. *Entomologisk Tidskrift*, 60: 1–28.

Misof B. Fleck G. 2003. Comparative analysis of mt LSU rRNA secondary structures of Odonates: Structural variability and phylogenetic signal. *Insect Molecular Biology* 12(6): 535–547.

Ma Y, Zheng BY, Zhu JC, Achterberg CV, Tang P, Chen XX. 2019. The first two mitochondrial genomes of wood wasps (Hymenoptera: Symphyta): Novel gene rearrangements and higher-level phylogeny of the basal hymenopterans. *International Journal of Biological Macromolecules* 123: 1189–1196.

Nawrocki EP. 2009. Structural RNA homology search and alignment using covariance models. *Washington University in St. Louis.*1–282.

Niu GY, Korkmaz EM, Doğan Ö, Zhang YY, Aydemir MN, Budak M, Du SY, Başıbüyük HH, Wei MC. 2018. The first mitogenomes of the superfamily Pamphilioidea (Hymenoptera: Symphyta): Mitogenome architecture and phylogenetic inference. *International Journal of Biological Macromolecules* 124: 185–199.

Niu GY, Zhang YY, Li ZY, Wei MC. 2019. Characterization of the mitochondrial genome of *Analcellicampa xanthosoma* gen. et sp. nov. (Hymenoptera: Tenthredinidae). *PeerJ* DOI.org/10.7717/peerj.6866.

Perna NT, Kocher TD. 1995. Patterns of nucleotide composition at fourfold degenerate sites of animal mitochondrial genomes. *Journal of Molecular Evolution* 41: 353–358.

Peng Y, Chen B, LI TJ. 2017. Sequencing and analysis of the complete mitochondrial genome of *Parapolybia crocea* (Hymenoptera:Vespidae). *Acta Entomologica Sinicus* 60(4): 464–474.

Peters RS, Krogmann L, Mayer C, Donath A, Gunkel S, Meusemann K, Kozlov A, Podsiadlowski L, Petersen M, Lanfear R, Diez PA, Heraty J, Kjer KM, Klopfstein S, Meier R, Polidori C. Schmitt T. Liu S, Zhou X, Wappler T, Rust J, Misof B, Niehuis O. 2017. Evolutionary history of the Hymenoptera, *Current Biology* 27: 1–6.

Ronquist F, Teslenko M, Van Der Mark P, Ayres DL, Darling A, Höhna S, Larget B, Liu L, Suchard M a, Huelsenbeck JP. 2012. Mrbayes 3.2: Efficient bayesian phylogenetic inference and model choice across a large model space. *Systematic Biology* 61: 539–542.

Ross HH. 1937. A Generic Classification of the Nearctic Sawflies (Hymenoptera: Symphyta). *Illinois biological monographs* Urbana 15(2): 1–173.

769 Ross HH. 1945. Sawfly genitalia: terminology and study techniques. *Entomological News*
770 61(10): 261–268.
771 Song SN, Tang P, Wei SJ, Chen XX. 2016. Comparative and phylogenetic analysis of the
772 mitochondrial genomes in basal hymenopterans. *Scientific Reports* 6(1): 20972–20972.
773 Song SN, Wang ZH, Li Y, Wei SJ, Chen XX. 2015. The mitochondrial genome of *Tenthredo*
774 *tienmushana* (Takeuchi) and a related phylogenetic analysis of the sawflies (Insecta:
775 Hymenoptera). *Mitochondrial DNA*: 1–2.
776 Schmidt S, Walter GH, Grigg J, Moore CJ. 2006. Sexual communication and host plant
777 associations of Australian pergid sawflies (Hymenoptera: Symphyta: Pergidae). *Recent Sawfly*
778 *Research: Synthesis and Prospevts*, pages 173–194.
779 Schmidt S, Walter GH. 2014. Young clades in an old family: major evolutionary transitions and
780 diversification of the eucalypt feeding pergid sawflies in Australia (Insecta, Hymenoptera,
781 Pergidae). *Molecular Phylogenetics and Evolution*74: 111–121.
782 Sharkey MJ, Carpenter JM, Vilhelmsen L, Heraty J, Dowling APG, Schulmeister S, Murray D,
783 Andrew R, Ronquist F, Krogmann L, Wheeler WC. 2012. Phylogenetic relationships among
784 superfamilies of Hymenoptera. *Cladistics* 28: 80–112.
785 Siebert S, Backofen R. 2005. MARNA: multiple alignment and consensus structure prediction of
786 RNAs based on sequence structure comparisons. *Bioinformatics* 21: 3352.
787 Schulmeister S.2003. Simultaneous analysis of basal Hymenoptera (Insecta): introducing robust-
788 choice sensitivity analysis. *Biological Journal of the Linnean Society. Linnean Society of*
789 *London*79: 245–275.
790 Taeger A, Blank SM, Liston AD. 2010. World catalog of Symphyta (Hymenoptera). *Zootaxa*
791 2580: 1–1064.
792 Takeuchi K. 1952. A generic Classification of the Japanese Tenthredinidae (Hymenoptera:
793 Symphyta). *Kyoto* 1–90.
794 Tang P, Zhu JC, Zheng BY, Wei SJ, Sharkey MJ, Chen XX, Vogler AP. 2019. Mitochondrial
795 phylogenomics of the Hymenoptera. *Molecular Phylogenetics and Evolution* 131: 8–18.
796 Vaidya G, Lohman DJ, Meier R. 2011. Sequence Matrix: Concatenation software for the fast
797 assembly of multi-gene datasets with character set and codon information. *Cladistics* 27: 171–
798 180.
799 Viitasaari M. 2002. Sawflies (Hymenoptera, Symphyta) I. A review of the suborder, the Western
800 Palaearctic taxa of Xyeloidea and Pamphilioidea. Helsinki *Tremex* Press Ltd. Finland. 1–164.
801 Vilhelmsen L. 1997. The phylogeny of lower Hymenoptera (Insecta), with a summary of the
802 early evolutionary history of the order. *Journal of Zoological Systematics and Evolutionary*
803 *Research* 35: 49–70.
804 Vilhelmsen L. 2001. Phylogeny and classification of the extant basal lineages of the
805 Hymenoptera (Insecta), *Zoological Journal of the Linnean Society* 131:393–442.
806 Vilhelmsen L.2015. Morphological phylogenetics of the Tenthredinidae (Insecta: Hymenoptera).
807 *Invertebrate Systematics* 29:164–190.

Vilhelmsen L. 2019. Giant sawflies and their kin: morphological phylogeny of Cimbicidae (Hymenoptera). *Systematic Entomology*, 44:103–127.
Wei MC. Nie HY.1997. Preliminary phylogeny of Symphyta (Hymenoptera). *Journal of Central South Forestry University*, 17(1):36–41.
Wei SJ, Niu FF, and Du BZ. 2014. Rearrangement of *trnQ-trnM* in the mitochondrial genome of *Allantus luctifer* (Smith) (Hymenoptera: Tenthredinidae). *Mitochondrial DNA Part A,* 27(2):856–858.
Wei SJ, Wu QL, Liu W. 2015. Sequencing and characterization of the *Monocellicampa pruni* (Hymenoptera: Tenthredinidae) mitochondrial genome. *Mitochondrial DNA* 26:157–158.
Wei SJ, Shi M, Chen XX, Sharkey MJ, Achterberg CV, Ye GY, He JH. 2010. New views on strand asymmetry in insect mitochondrial genomes. *PlosOne*, 5(9):1–10.
Wolstenholme DR. 1992. Animal mitochondrial DNA: structure and evolution. *International Review of Cytology* 141:173.
Wu QL, Li Q, Gu Y, Shi BC, van Achterberg C, Wei SJ, Chen XX. 2014. The complete mitochondrial genome of *Taeniogonalos taihorina* (Bischoff) (Hymenoptera: Trigonalyidae) reveals a novel gene rearrangement pattern in the Hymenoptera. *Gene* 543:76–84.
Yan YC, Niu GY, Lan BC, Wei MC. 2018. Review of *Leptocimbex formosanus* group (Hymenoptera: Cimbicidae) with two new Chinese species, *Entomological Research* 48: 372–383.
Yan YC, Wei MC. 2010. The first record of *Orientabia* malaise from China with description of a new species (Hymenoptera, Cimbicidae). *Acta Zootaxonomica Sinicus* 35 (3): 627–630.
Yan YC, Wei MC. 2013. A new species of the genus *Leptocimbex* Semenov-Tian-Shanskij (Hymenoptera, Cimbicidae) from Hunan, China. *Acta Zootaxonomica Sinicus* 38: 130–133.
Yan YC, Wei MC. 2016. A new species and a new record of *Leptocimbex* Semenov (Hymenoptera: Cimbicidae) from China. *Entomotaxonomia* 38: 227–234.
Yan YC, Xiao W, Wei MC. 2014. Two new species of *Leptocimbex* Semenov (Hymenoptera: Cimbicidae) from China. *Entomotaxonomia* 36: 311–320.
Zhao Y, Zhang H, Zhang Y. 2017. Complete mitochondrial genome of *Neochauliodes parasparsus* (Megaloptera: Corydalidae) with phylogenetic consideration. *Biochemical Systematics & Ecology* 70:192–199.

Notes

Table 1. Summary information of symphytan mitochondrial genomes used in phylogenetic analyses.

Table 2. The partitions of the mitochondrial genome sequences identified by PartitionFinder.

Table 3. Mitochondrial genome characteristics of *L. sinicus*.

Table 4. Nucleotide composition of *L. sinicus* mitochondrial genome.

Table 5. Codon usage of PCGs in mitochondrial genome of *L. sinicus*. No., frequency of each codon; RSCU, relative synonymous condon usage.

Figure 1. *Labriocimbex sinicus* Yan & Wei sp. nov.
A. Adult female (holotype), dorsal view; B. Adult male (paratype), dorsal view. Scale bar = 2 mm.

Figure 2. *Labriocimbex sinicus* Yan & Wei, gen. et sp. nov.
A. Head of female, front view; B. Head of female, lateral view; C. Mesopleuron of female, lateral view; D. Head of female, dorsal view; E. Metanotum and base of abdomen; F. Abdomen, lateral view; G. Palpus; H. Antenna of female.

Figure 3. *Labriocimbex sinicus* Yan & Wei, gen. et sp. nov.
A. Left mandible; B. Right mandible; C. Femur of hind leg; D. Ovipositor sheath of female, lateral view; E. Genital plate of male, ventral view; F. Ovipositor sheath of female, dorsal view; G. Middle serrulae, Scale bar = 50 um; H. Penis valve; I. Gonoforcep. J. Spur of hind tibia; K. Claw; L. Apex of abdomen, ventral view; M. Lance; N. Lancet (H, I, M and N, Scale bar = 200 um).

Figure 4. *Labriocimbex zaraeoides* (Malaise, 1939) comb. nov.
A. Adult female (holotype), Scale bar = 2 mm; B. Mesopleuron of female, lateral view; C. Head of female, front view; D. Abdomen, lateral view; E. Head of female, dorsal view; F. Head of female, lateral view; G. Metanotum and basal of abdominal terga, dorsal view; H. Labels.

Figure 5. Mitochondrial genome organization of three cimbicid species referenced with the ancestral insect mitochondrial genomes. Genes transcribed from the J and N strands are shown with green and orange color, respectively. Overlapping and intergenic regions are marked in yellow and blue circles. tRNA genes are denoted by a one-letter symbol according to the IPUC-IUB single-letter amino acid codes A+ T-rich region is marked in blue and tRNA genes are labelled by the single-letter amino acid code.
A. Ancestral type of insect mitochondrial genomes; B. *Corynis laterlis* mitochondrial genomes; C. *Trichiosoma anthracinum* mitochondrial genomes; D. *Labriocimbex sinca* mitochondrial genomes.

Figure 6. Predicted secondary structures for the 22 typical tRNA genes of *L. sinicus* and *T. anthracinum* mitogenomes. Base-pairing is indicated as follows: Watson–Crick pairs by lines, wobble GU pairs by dots and other noncanonical pairs by circles. Variable regions are presented in boxes with red (*L. sinicus*) and blue (*T. anthracinum*) color.
A. *trnA*; B. *trnR*; C. *trnN*; D. *trnD*; E. *trnC*; F. *trnQ*; G. *trnE*; H. *trnG*; I. *trnH*; J. *trnI*; K. *trnL1*; L. *trnL2*; M. *trnK*; N. *trnM*; O. *trnF*; P. *trnP*; Q. *trnS1*; R. *trnS2*; S. *trnT*; T. *trnW*; U. *trnY*; V. *trnV*.

Figure 7. Predicted secondary structures for the 22 tRNA genes of C. *lateralis.* Dashes indicate Watson-Crick base pairing and dots indicate G-U base pairing.
A. *trnA*; B. *trnR*; C. *trnN*; D. *trnD*; E. *trnC*; F. *trnQ*; G. *trnE*; H. *trnG*; I. *trnH*; J. *trnI*; K. *trnL1*; L. *trnL2*; M. *trnK*; N. *trnM*; O. *trnF*; P. *trnP*; Q. *trnS1*; R. *trnS2*; S. *trnT*; T. *trnW*; U. *trnY*; V. *trnV*.

Figure 8. The predicted secondary structures of *rrnL* of *L. sinicus* and *T. anthracinum.*
Tertiary interactions and base triples are connected by continuous lines. The numbering of helix follows Gillespie et al. (2006). Roman numbers refer to domain names. Dashes indicate Watson-Crick base pairing and dots indicate G-U base pairing. The helical variation among cimbicid species are presented in boxes with red (*L. sinicus*) and blue (*T. Anthracinum*) color.

Figure 9. *Corynis lateralis rrnL*.
Predicted *rrnL* secondary structure in *C. lateralis.* The numbering of helix follows Gillespie et al. (2006).Roman numbers refer to domain names.

Figure 10. The predicted secondary structures of *rrnS* of *L. sinicus* and *T. anthracinum.*
Tertiary interactions and base triples are connected by continuous lines. The numbering of helix follows Gillespie et al. (2006). Roman numbers refer to domain names. Dashes indicate Watson-Crick base pairing and dots indicate G-U base pairing. The helical variation among cimbicid species are presented in boxes with red (*L. sinicus*) and blue (*T. anthracinum*) color.

Figure 11. *Corynis lateralis rrnS*.
Predicted *rrnS* secondary structure in *C. lateralis.* The numbering of helix follows Gillespie et al. (2006). Roman numbers refer to domain names.

Figure 12. The phylogenetic tree of Symphyta from iqtree analysis.
Phylogenetic tree of Symphyta, based on ML analysis of the 13 PCGs (*ND2*, *COXI1*, *COX2*, *ATP8*, *ATP6*, *COX3*, *ND3*, *ND5*, *ND4*, *ND4L*, *ND6*, *CYT8*, and *ND1*) and 2 rRNAs (*rrnL* and *rrnS*) data set. Values branches represent maximum likelihood bootstrap clade frequency (CF) support. The scale bar indicates the number of substitutions per site.

Figure 13. The phylogenetic tree of Symphyta from Bayesian analysis.
Phylogenetic tree of Symphyta, based on BI analysis of the 13 PCGs (*ND2*, *COXI1*, *COX2*, *ATP8*, *ATP6*, *COX3*, *ND3*, *ND5*, *ND4*, *ND4L*, *ND6*, *CYT8*, and *ND1*) and 2 rRNAs (*rrnL* and *rrnS*) data set. Values branches represent BI posterior probability (PP) support. The scale bar indicates the number of substitutions per site.

Table 1(on next page)

Summary information of symphytan mitochondrial genomes used in phylogenetic analyses.

	Species	Family	Accesion number	References
Ingroup	*Labriocimbex sinicus*	Cimbicidae	MH136623	this study
	Corynis lateralis	Cimbicidae	KY063728	Doğan and Korkmaz, 2017
	Trichiosoma anthracinum	Cimbicidae	KT921411	Song *et al*., 2016
	Megalodontes cephalotes	Megalodontesidae	MH577058	Niu *et al*., 2018
	Megalodontes spiraeae	Megalodontesidae	MH577059	Niu *et al*., 2018
	Megalodontes quinquecinctus	Megalodontesidae	MG923502	Tang *et al*., 2019
	Analcellicampa xanthosoma	Tenthredinidae	MH992752	Niu *et al*., 2019
	Allantus luctifer	Tenthredinidae	KJ713152	Wei *et al*., 2014
	Asiemphytus rufocephalus	Tenthredinidae	KR703582	Song *et al*., 2016
	Monocellicampa pruni	Tenthredinidae	JX566509	Wei *et al*., 2015
	Tenthredo tienmushana	Tenthredinidae	KR703581	Song *et al*., 2015
	Birmella discoidalisa	Tenthredinidae	MF197548	Unpublished
	Xyela sp.	Xyelidae	MG923517	Tang *et al*., 2019
	Xiphydria sp.	Xiphydriidae	MH422969	Ma *et al*., 2018
	Tremex columba	Siricidae	MH422968	Ma *et al*., 2018
	Pamphilius sp.	Pamphiliidae	MG923504	Tang *et al*., 2019
	Chinolyda flagellicornis	Pamphiliidae	MH577057	Niu *et al*., 2018
	Orussus occidentalis	Orussidae	FJ478174	Dowton *et al*., 2009
	Arge similes	Argidae	MG923484	Tang *et al*., 2019
	Arge bella	Argidae	MF287761	Du *et al*., 2018
	Calameuta filiformis	Cephidae	KT260167	Korkmaz *et al*., 2016
	Calameuta idolon	Cephidae	KT260168	Korkmaz *et al*., 2016
	Cephus cinctus	Cephidae	FJ478173	Dowton *et al*., 2009
	Cephus pygmeus	Cephidae	KM377623	Korkmaz *et al*., 2015
	Cephus sareptanus	Cephidae	KM377624	Korkmaz *et al*., 2015
	Characopygus scythicus	Cephidae	KX907848	Korkmaz *et al*., 2018
	Hartigia linearis	Cephidae	KX907843	Korkmaz *et al*., 2018
	Janus compressus	Cephidae	KX907844	Korkmaz *et al*., 2018
	Pachycephus cruentatus	Cephidae	KX907845	Korkmaz *et al*., 2018
	Pachycephus smyrnensis	Cephidae	KX907846	Korkmaz *et al*., 2018
	Syrista parreyssi	Cephidae	KX907847	Korkmaz *et al*., 2018
	Trachelus iudaicus	Cephidae	KX257357	Korkmaz *et al*., 2017
	Trachelus tabidus	Cephidae	KX257358	Korkmaz *et al*., 2017
	Perga condei	Pergidae	AY787816	Castro and Dowton, 2005
	Taeniogonalos taihorina	Trigonalidae	NC027830	Wu *et al*., 2014
	Parapolybia crocea	Vespidae	KY679828	Peng *et al*., 2017
Outgroup	*Paroster microsturtensis*	Dytiscidae	MG912997	Hyde *et al*., 2018
	Neopanorpa phlchra	Panorpidae	FJ169955	Unpublished
	Neochauliodes parasparsus	Corydalidae	KX821680	Zhao *et al*., 2017
	Anopheles gambiae	Culicidae	L20934	Beard *et al*., 1993

1

Table 2(on next page)

The partitions of the mitochondrial genome sequences identified by PartitionFinder.

1

Partitions	Best Models	sites	genes
P1	GTR+I+G	1568	*rrnS*
P2	GTR+I+G	2032	*rrnL*
P3	GTR+I+G	751	*ND3*_1st, *ATP6*_1st, *CYTB*_1st
P4	GTR+I+G	1784	*ND3*_2nd, *ATP6*_2nd, *COX3*_2nd, *CYTB*_2nd, *COX2*_2nd, *COX1*_2nd
P5	GTR+I+G	1849	*ND3*_3rd, *COX2*_3rd, *ATP8*_3rd, *ATP6*_3rd, *COX1*_3rd, *COX3*_3rd, *CYTB*_3rd
P6	F81+G	130	*ATP8*_1st, *ATP8*_2nd
P7	GTR+I+G	522	*COX1*_1st
P8	GTR+I+G	511	*COX3*_1st, *COX2*_1st
P9	GTR+I+G	906	*ND4L*_1st, *ND4*_1st, *ND1*_1st
P10	GTR+I+G	906	*ND4*_2nd, *ND1*_2nd, *ND4L*_2nd
P11	GTR+G	906	*ND1*_3rd, *ND4*_3rd, *ND4L*_3rd
P12	GTR+I+G	599	*ND6*_1st, *ND2*_1st
P13	GTR+I+G	599	*ND6*_2nd, *ND2*_2nd
P14	GTR+G	599	*ND6*_3rd, *ND2*_3rd
P15	GTR+G	604	*ND5*_1st
P16	GTR+G	604	*ND5*_2nd
P17	HKY+G	603	*ND5*_3rd

Table 3(on next page)

Mitochondrial genome characteristics of *L. sinicus*.

1

Gene	Strand	Start	Stop	Length(bp)	Start codon	Stop codon	Anticodon	IGN
trnI	J	1	67	67			GAU	1
ND2	J	70	1113	1044	ATG	TAA		2
trnW	J	1117	1181	65			UCA	3
COI	J	1182	2720	1539	ATT	TAA		0
trnL2	J	2760	2825	66			UAA	39
COII	J	2827	3510	684	ATG	TAA		1
trnK	J	3532	3602	71			CUU	21
trnD	J	3603	3672	70			GUC	0
ATP8	J	3673	3834	162	ATC	TAA		0
ATP6	J	3828	4517	690	ATG	TAA		-7
COIII	J	4504	5289	786	ATG	TAA		-14
trnG	J	5310	5373	64			UCC	20
ND3	J	5374	5724	351	ATT	TAA		0
trnA	J	5732	5797	66		T	UGC	7
trnR	J	5798	5,864	67			UCG	0
trnN	J	5,866	5,934	69			GUU	1
trnS1	J	5,935	6,002	68			UGA	0
trnE	J	6,010	6,076	67			UUC	7
trnF	N	6,092	6158	67			AAG	15
ND5	N	6,159	7872	1714	ATT	T		0
trnH	N	7873	7940	68			GUG	0
ND4	N	7991	9343	1353	ATT	TAA		50
ND4L	N	9337	9618	282	ATT	TAA		-7
trnT	N	9621	9865	65			UGU	2
trnP	N	9686	9751	66			GGU	0
ND6	J	9753	10256	504	ATA	TAA		1
CYTB	J	10258	11391	1134	ATA	TAA		1
trnS2	J	11435	11502	68			UCU	43
ND1	N	11512	12462	951	ATT	TAA		9
trnL1	N	12463	12530	68			GAU	0
rrnL	N	12531	13871	1341				0
trnV	N	13872	13941	70			CAU	0
rrnS	N	13941	14731	791				-1

trnM	J	14777	14845	69	CAU	45
trnQ	N	14843	14911	69	GUU	-3
CR	none	14912	15261	350		0
trnY	J	15262	15331	70	GUA	0
trnC	N	15333	15403	71	ACG	1

2
3

Table 4(on next page)

Nucleotide composition of *L. sinicus* mitochondrial genome.

1

Feature	Length(bp)	A%	C%	G%	T%	A+T%	AT-skew	GC-skew
Whole genome	15405	43.5	11.1	7.7	37.7	81.2	0.0714	-0.1809
Protein coding genes	12456	34.4	9.7	10.4	45.5	79.9	-0.1389	0.0348
First codon position	4152	36.9	9.5	15.1	38.5	75.4	-0.0212	0.2276
Second codon position	4152	20.9	16.2	13	49.9	70.8	-0.4096	-0.1096
Third codon position	4152	45.5	3.5	3	48	93.5	-0.0267	-0.0769
Protein coding genes-J	6840	37.8	12	9.3	40.9	78.7	-0.0394	-0.1268
First codon position	2280	40.4	11.9	14.6	33.1	73.5	0.0993	0.1019
Second codon position	2280	23	18.7	12	46.3	69.3	-0.3362	-0.2182
Third codon position	2280	50	5.3	1.4	43.3	93.3	0.0718	-0.5821
Protein coding genes-N	5616	30.3	7	11.6	51.1	81.4	-0.2555	0.2473
First codon position	1872	32.5	6.7	15.6	45.2	77.7	-0.1634	0.3991
Second codon position	1872	18.4	13.1	14.3	54.3	72.7	-0.4938	0.0438
Third codon position	1872	40.1	1.2	5	53.7	93.8	-0.1450	0.6129
ATP6	690	38.3	11.2	8	42.6	80.9	-0.0532	-0.1667
ATP8	162	45.1	9.3	2.5	43.2	88.3	0.0215	-0.5763
ND1	951	51.4	12.3	6.9	29.3	80.7	0.2739	-0.2813
ND2	1044	44.1	9.9	5.7	40.3	84.4	0.0450	-0.2692
ND3	351	35	10.5	9.7	44.7	79.7	-0.1217	-0.0396
ND4	1353	51.2	11.5	7.4	29.9	81.1	0.2626	-0.2169
ND4-BLASTP	1344	51.3	11.6	7.4	29.7	81	0.2667	-0.2211
ND4L	282	49.6	12.1	3.5	34.8	84.4	0.1754	-0.5513
ND5	1714	50.8	11.1	6.8	31.3	82.1	0.2375	-0.2402
ND6	504	42.1	8.7	5	44.2	86.3	-0.0243	-0.2701

COI	1539	35.1	13.5	12.8	38.7	73.8	-0.0488	-0.0266
COII	684	40.8	12.7	8	38.5	79.3	0.0290	-0.2271
COIII	786	33.5	13	12	41.6	75.1	-0.1079	-0.0400
CYTB	1134	35.4	13.1	10.4	41.2	76.6	-0.0757	-0.1149
12s	791	44	10.7	5.3	40.1	84.1	0.04637337	0.3375
16s	1341	46.8	11	4.9	37.4	84.2	0.111639	-0.383648

Table 5(on next page)

Codon usage of PCGs in mitochondrial genome of *L. sinicus.* No., frequency of each codon; RSCU, relative synonymous condon usage.

1

Amino acid	Codon	NO.	RSCU		Amino acid	Codon	NO.	RSCU	
Phe	TTT	409	1.9		Tyr	TAT	159	1.78	
	TTC	21	0.1	2		TAC	20	0.22	2
Leu	TTA	560	5.04		End	TAA	0	0	
	TTG	35	0.31	5.35		TAG	0	0	
Leu	CTT	37	0.33		His	CAT	68	1.79	
	CTC	0	0			CAC	8	0.21	2
	CTA	34	0.31	6	Gln	CAA	61	1.85	
	CTG	1	0.01	0.65		CAG	5	0.15	2
Ile	ATT	464	1.87		Asn	AAT	237	1.84	
	ATC	31	0.13	2		AAC	20	0.16	2
Met	ATA	314	1.91		Lys	AAA	135	1.88	
	ATG	15	0.09	2		AAG	9	0.13	2.01
Val	GTT	83	2.21		Asp	GAT	62	1.82	
	GTC	1	0.03			GAC	6	0.18	2
	GTA	65	1.73		Glu	GAA	72	1.85	
	GTG	1	0.03	4		GAG	6	0.15	2
Ser	TCT	134	2.67		Cys	TGT	37	1.95	
	TCC	4	0.08			TGC	1	0.05	2
	TCA	116	2.31		Trp	TGA	92	1.8	
	TCG	2	0.04	5.1		TGG	10	0.2	2
Pro	CCT	64	1.97		Arg	CGT	20	1.54	
	CCC	15	0.46			CGC	0	0	

	CCA	48	1.48			CGA	31	2.38	
	CCG	3	0.09	4		CGG	1	0.08	4
Thr	ACT	70	1.74		Ser	AGT	23	0.46	
	ACC	8	0.2			AGC	1	0.02	
	ACA	82	2.04			AGA	119	2.37	
	ACG	1	0.02	4		AGG	2	0.04	2.89
Ala	GCT	65	2.08		Gly	GGT	62	1.22	
	GCC	7	0.22			GGC	1	0.02	
	GCA	49	1.57			GGA	112	2.2	
	GCG	4	0.13	4		GGG	29	0.57	4.01

Figure 1

Labriocimbex sinicus Yan & Wei sp. nov.

(A) Adult female (holotype), dorsal view; (B) Adult male (paratype), dorsal view. Scale bar = 2 mm.


A
B

Figure 2

Labriocimbex sinicus Yan & Wei, gen. et sp. nov.

(A) Head of female, front view; (B) Head of female, lateral view; (C) Mesopleuron of female, lateral view; (D) Head of female, dorsal view; (E) Metanotum and base of abdomen; (F) Abdomen, lateral view; (G) Palpus; (H) Antenna of female.

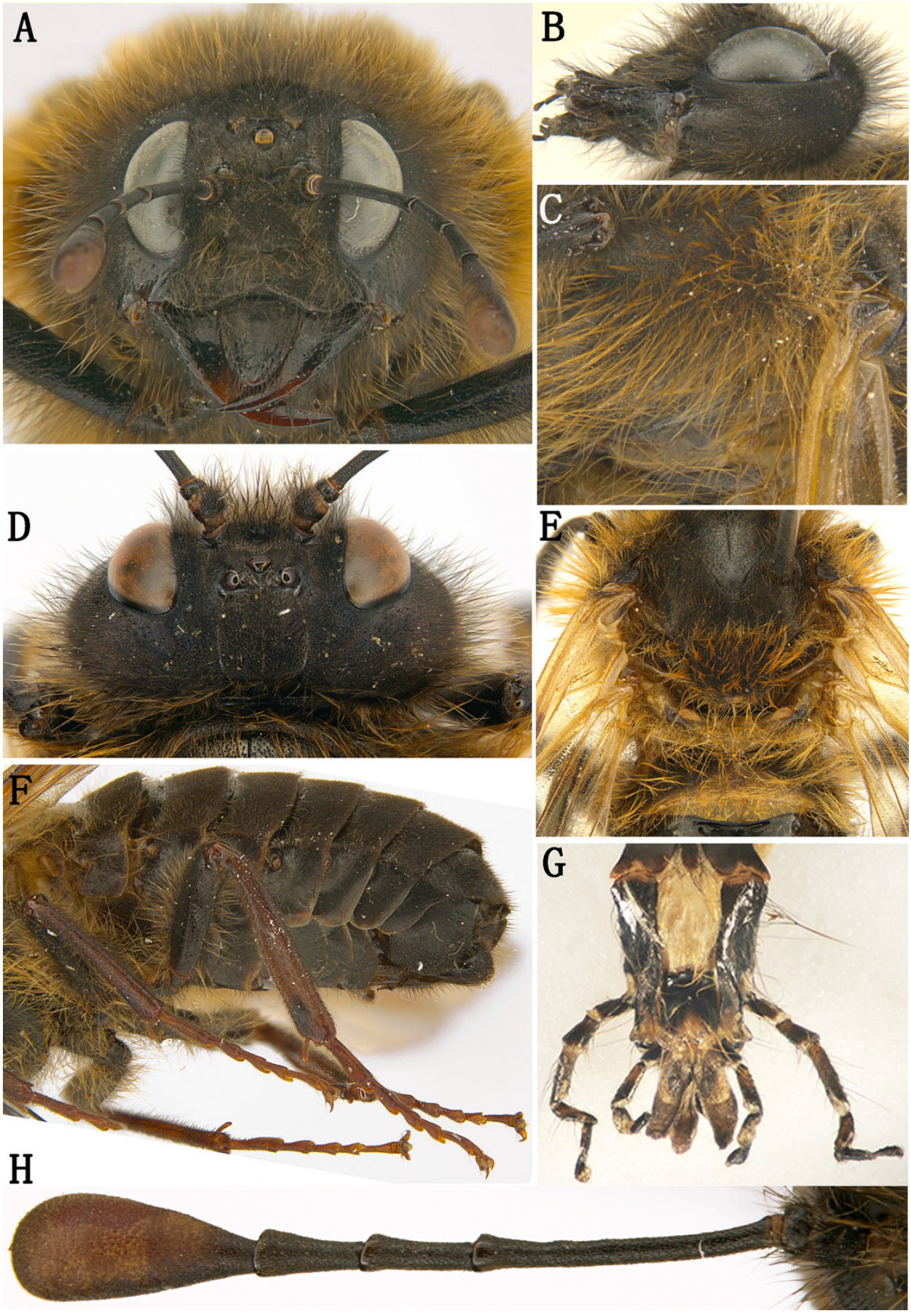
A
B
C
D
E
F
G
H

Figure 3

Labriocimbex sinicus Yan & Wei, gen. et sp. nov.

(A) Left mandible; (B) Right mandible; (C) Femur of hind leg; (D) Ovipositor sheath of female, lateral view; (E) Genital plate of male, ventral view; (F) Ovipositor sheath of female, dorsal view, (G) Middle serrulae, Scale bar = 50 um; (H) Penis valve; (I) Gonoforcep; (J) Spur of hind tibia; (K) Claw; (L) Apex of abdomen, ventral view; (M) Lance; (N) Lancet (H, I, M and N, Scale bar = 200 um).

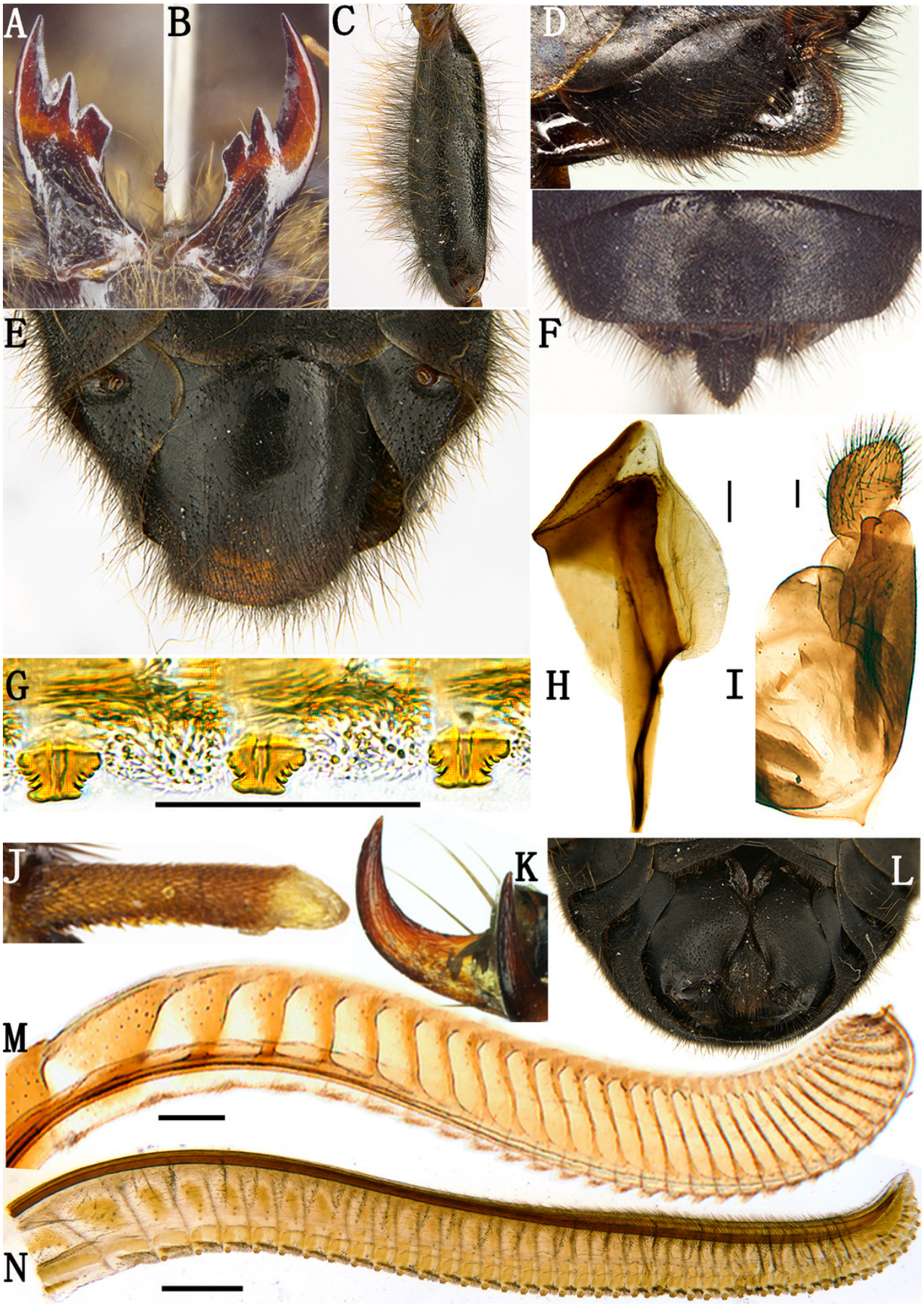
A
B
C
D
E
F
G
H
I
J
K
L
M
N

Figure 4

Labriocimbex zaraeoides (Malaise, 1939) comb. nov.

(A) Adult female (holotype), Scale bar = 2 mm; (B) Mesopleuron of female, lateral view; (C) Head of female, front view; (D) Abdomen, lateral view; (E) Head of female, dorsal view; (F) Head of female, lateral view; (G) Metanotum and basal of abdominal terga, dorsal view; (H) Labels.

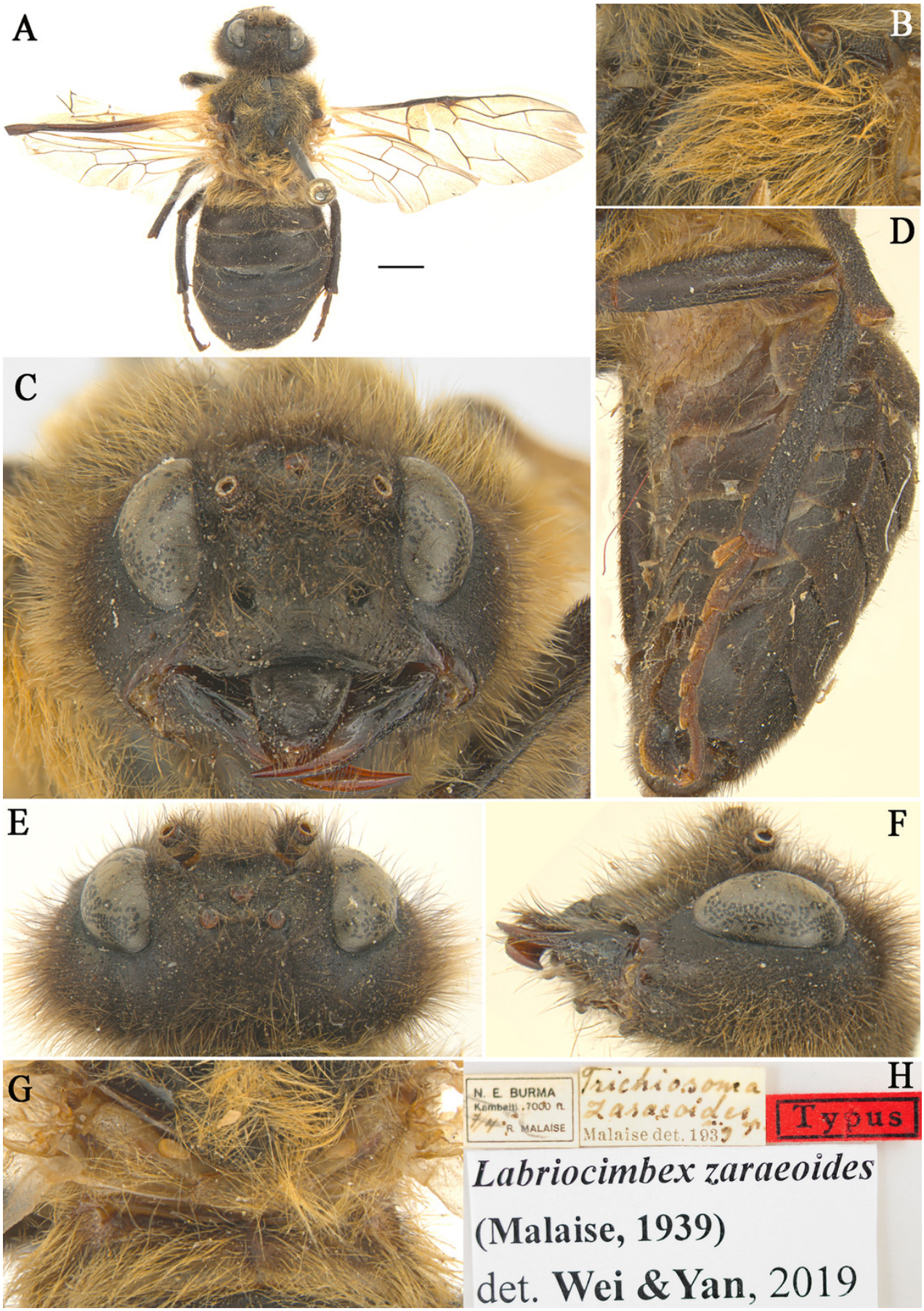
A
B
C
D
E
F
G
H
N. E. BURMA
Kambaiti, 7000 ft.
R. MALAISE
Trichiosoma
Zaraeoides
Malaise det. 193
Typus
Labriocimbex zaraeoides
(Malaise, 1939)
det. Wei &Yan, 2019

Figure 5

Mitochondrial genome organization of three cimbicid species referenced with the ancestral insect mitochondrial genomes.

Genes transcribed from the J and N strands are shown with green and orange color, respectively. Overlapping and intergenic regions are marked in yellow and blue circles. tRNA genes are denoted by a one-letter symbol according to the IPUC-IUB single-letter amino acid codes A+ T-rich region is marked in blue and tRNA genes are labelled by the single-letter amino acid code. (A) Ancestral type of insect mitochondrial genomes; (B) *Corynis laterlis* mitochondrial genomes; (C) *Trichiosoma anthracinum* mitochondrial genomes; (D) *Labriocimbex sinca* mitochondrial genomes.

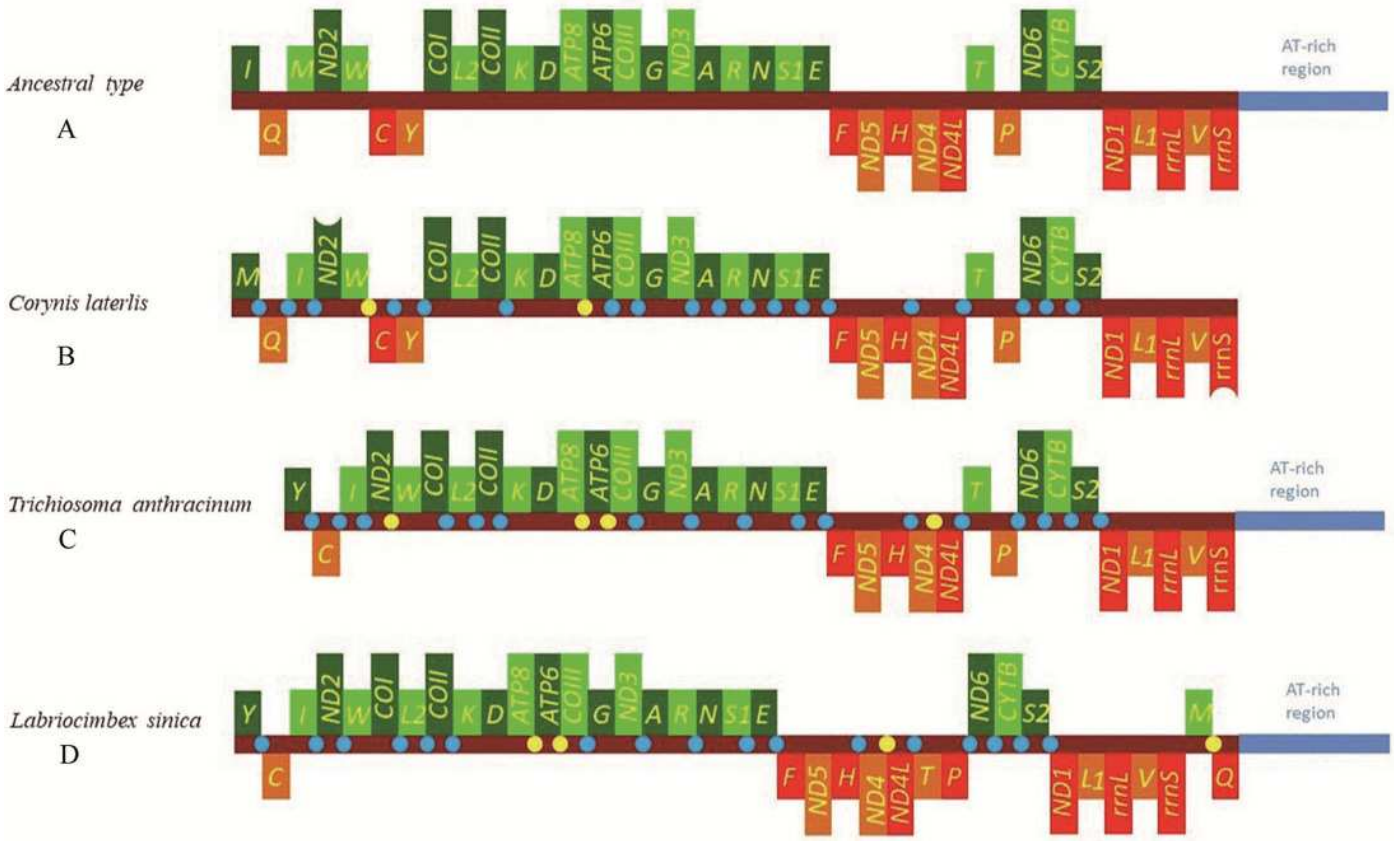

Figure 6

Predicted secondary structures for the 22 typical tRNA genes of *L. sinicus* and *T. anthracinum* mitogenomes.

Base-pairing is indicated as follows: Watson–Crick pairs by lines, wobble GU pairs by dots and other noncanonical pairs by circles. Variable regions are presented in boxes with red (*L. sinicus*) and blue (*T. anthracinum*) color . (A) *trnA*; (B) *trnR*; (C) *trnN*; (D) *trnD*; (E) *trnC*; (F) *trnQ*; (G) *trnE*; (H) *trnG*; (I) *trnH*; (J) *trnI*; (K) *trnL1*; (L) *trnL2*; (M) *trnK*; (N) *trnM*; (O) *trnF*; (P) *trnP*; (Q) *trnS1*; (R) *trnS2*; (S) *trnT*; (T) *trnW*; (U) *trnY*; (V) *trnV*.

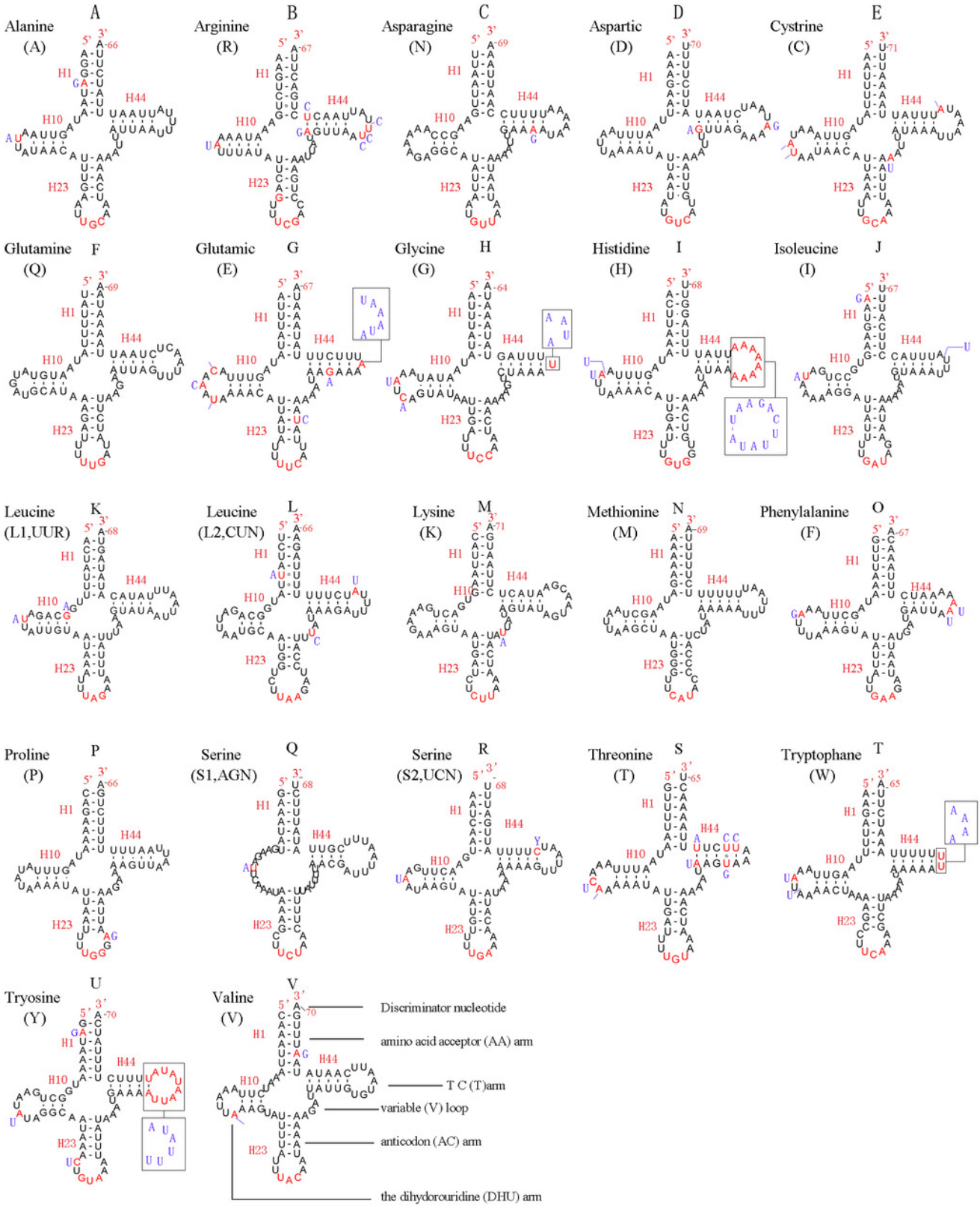
A
Alanine
(A)
B
Arginine
(R)
C
Asparagine
(N)
D
Aspartic
(D)
E
Cystrine
(C)
F
Glutamine
(Q)
G
Glutamic
(E)
H
Glycine
(G)
I
Histidine
(H)
J
Isoleucine
(I)
K
Leucine
(L1,UUR)
L
Leucine
(L2,CUN)
M
Lysine
(K)
N
Methionine
(M)
O
Phenylalanine
(F)
P
Proline
(P)
Q
Serine
(S1,AGN)
R
Serine
(S2,UCN)
S
Threonine
(T)
T
Tryptophane
(W)
U
Tryosine
(Y)
V
Valine
(V)
Discriminator nucleotide
amino acid acceptor (AA) arm
T C (T)arm
variable (V) loop
anticodon (AC) arm
the dihydorouridine (DHU) arm

Figure 7

Predicted secondary structures for the 22 tRNA genes of C*. lateralis.*

Dashes indicate Watson-Crick base pairing and dots indicate G-U base pairing. (A) *trnA*; (B) *trnR*; (C) *trnN*; (D) *trnD*; (E) *trnC*; (F) *trnQ*; (G) *trnE*; (H) *trnG*; (I) *trnH*; (J) *trnI*; (K) *trnL1*; (L) *trnL2*; (M) *trnK*; (N) *trnM*; (O) *trnF*; (P) *trnP*; (Q) *trnS1*; (R) *trnS2*; (S) *trnT*; (T) *trnW*; (U) *trnY*; (V) *trnV*.

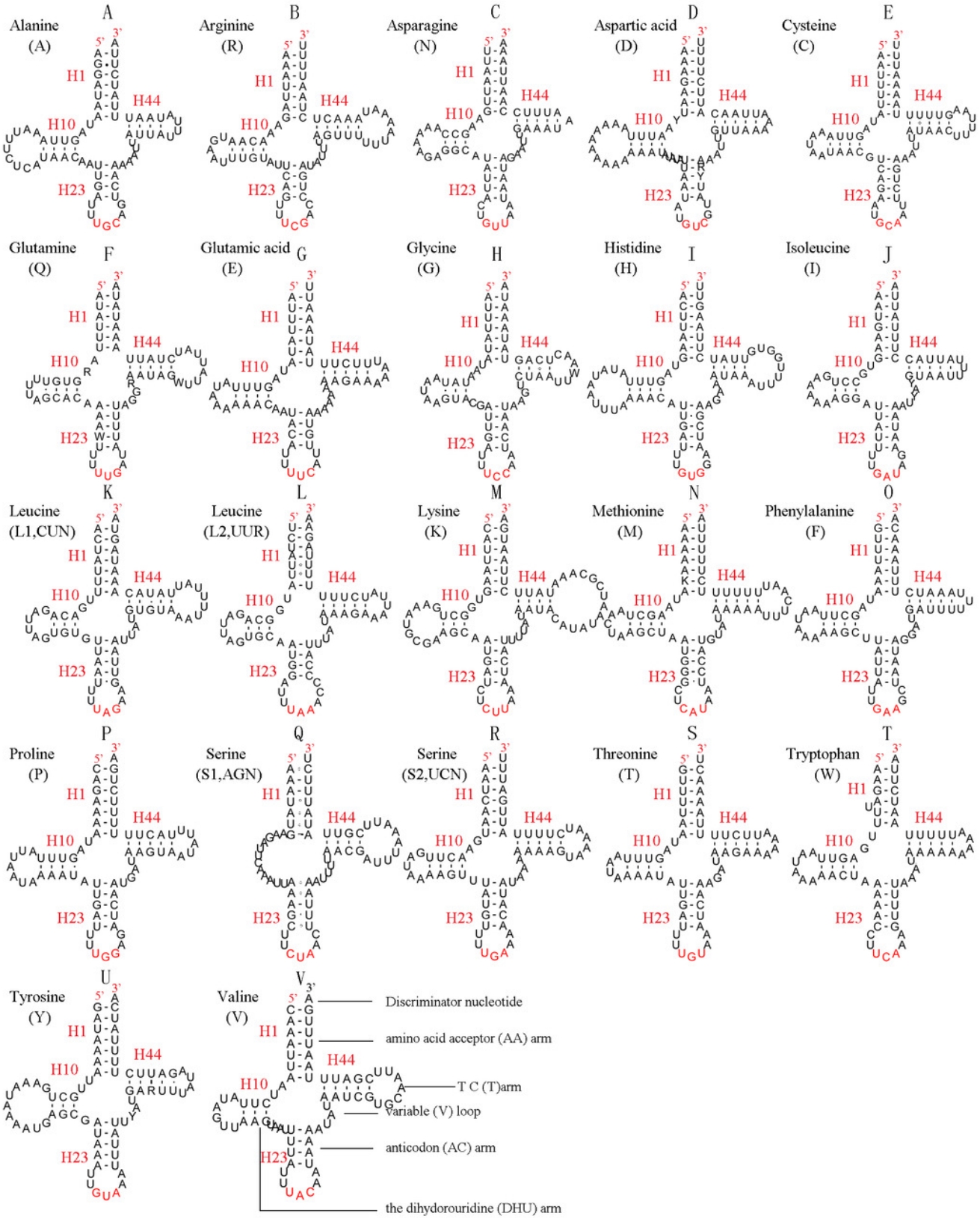
A
Alanine
(A)
B
Arginine
(R)
C
Asparagine
(N)
D
Aspartic acid
(D)
E
Cysteine
(C)
F
Glutamine
(Q)
G
Glutamic acid
(E)
H
Glycine
(G)
I
Histidine
(H)
J
Isoleucine
(I)
K
Leucine
(L1,CUN)
L
Leucine
(L2,UUR)
M
Lysine
(K)
N
Methionine
(M)
O
Phenylalanine
(F)
P
Proline
(P)
Q
Serine
(S1,AGN)
R
Serine
(S2,UCN)
S
Threonine
(T)
T
Tryptophan
(W)
U
Tyrosine
(Y)
V
Valine
(V)
H1
H10
H23
H44
5'
3'
Discriminator nucleotide
amino acid acceptor (AA) arm
T C (T)arm
variable (V) loop
anticodon (AC) arm
the dihydorouridine (DHU) arm

Figure 8

The predicted secondary structures of *rrnL* of *L. sinicus* and *T. anthracinum.*

Tertiary interactions and base triples are connected by continuous lines. The numbering of helix follows Gillespie et al. (2006). Roman numbers refer to domain names. Dashes indicate Watson-Crick base pairing and dots indicate G-U base pairing. The helical variation among cimbicid species are presented in boxes with red (*L. sinicus*) and blue (*T. Anthracinum*) color.

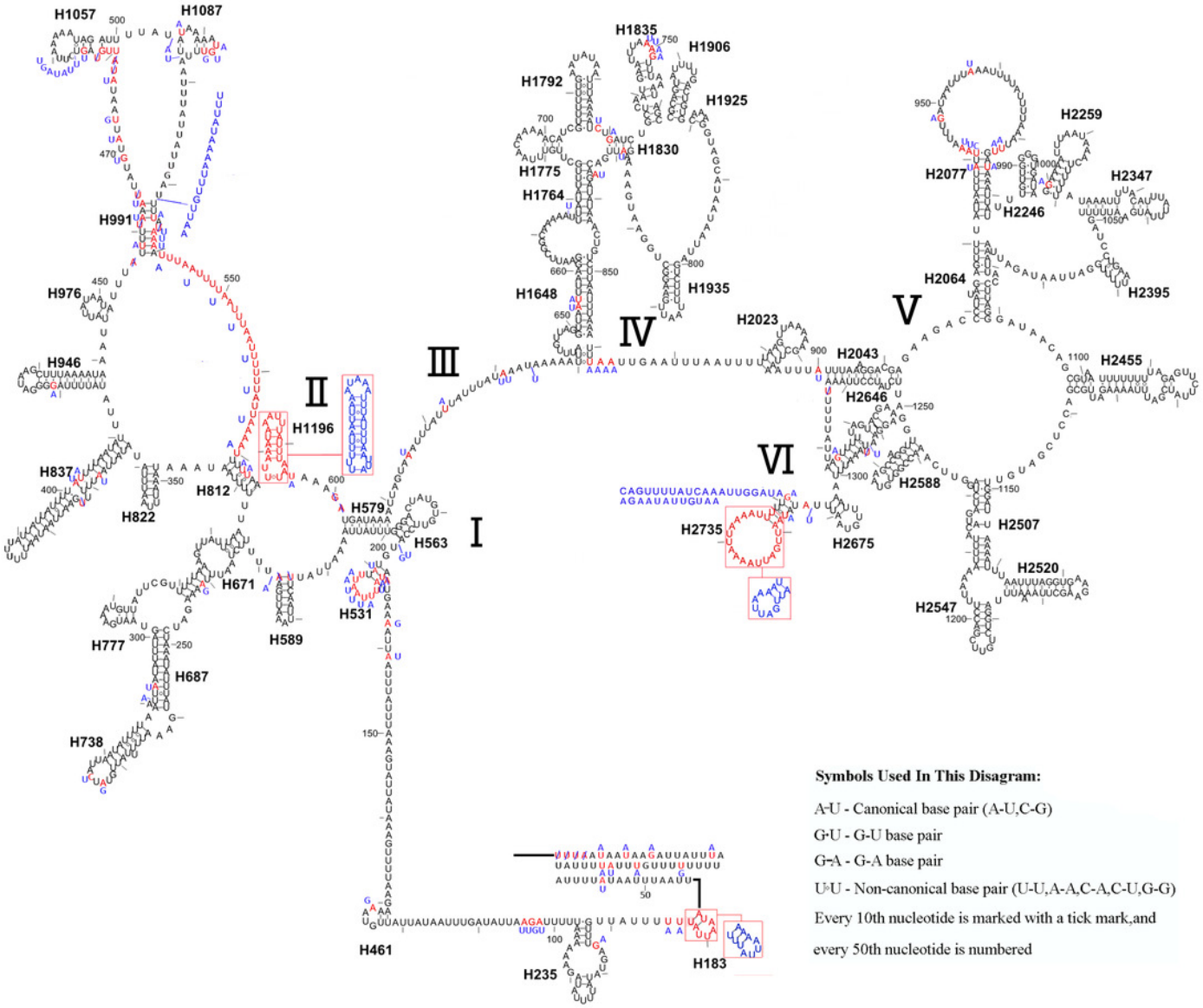

Figure 9

Corynis lateralis rrnL

Predicted *rrnL* secondary structure in *C. lateralis.* The numbering of helix follows Gillespie et al. (2006).Roman numbers refer to domain names.

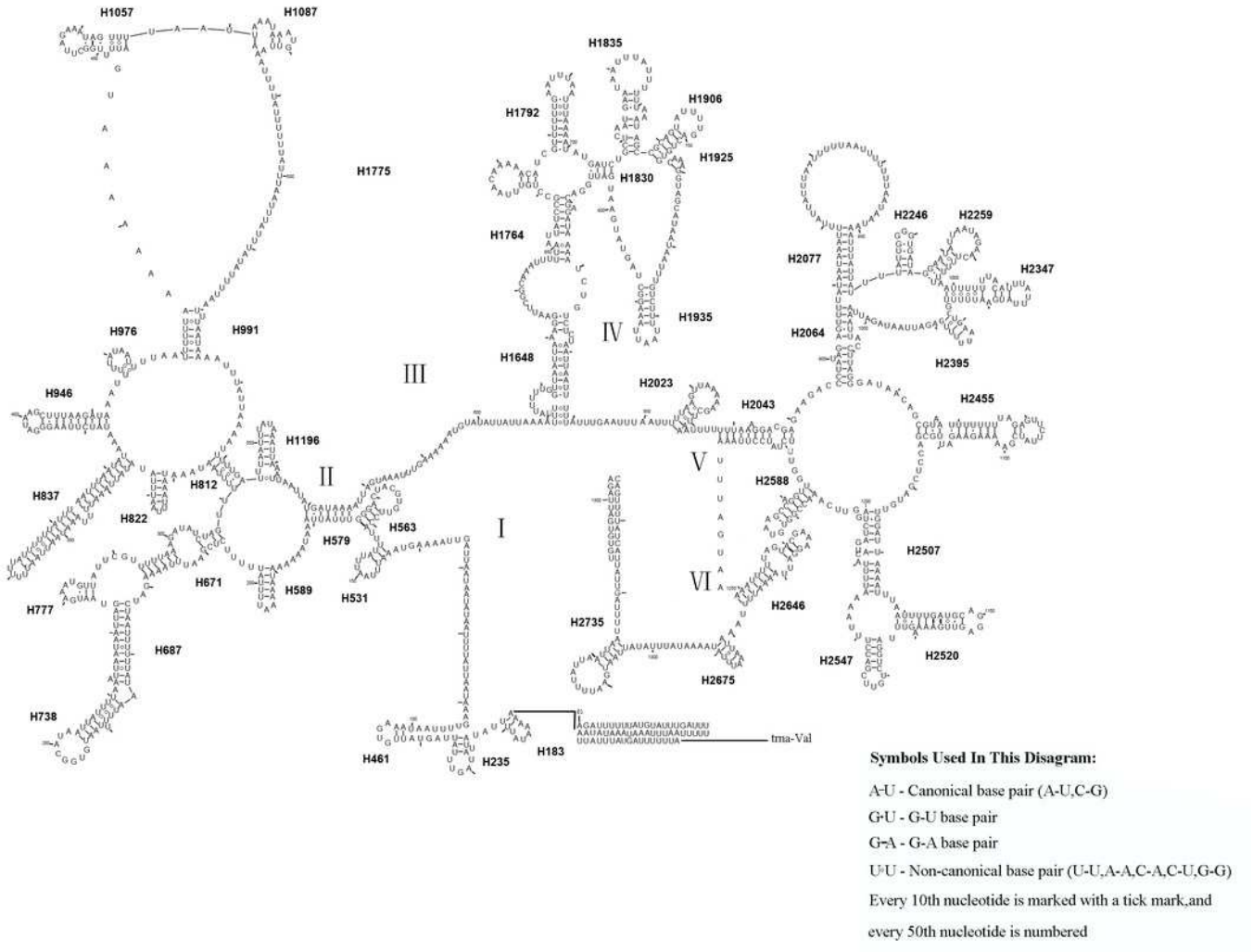

Figure 10

The predicted secondary structures of *rrnS* of *L. sinicus* and *T. anthracinum.*

Tertiary interactions and base triples are connected by continuous lines. The numbering of helix follows Gillespie et al. (2006). Roman numbers refer to domain names. Dashes indicate Watson-Crick base pairing and dots indicate G-U base pairing. The helical variation among cimbicid species are presented in boxes with red (*L. sinicus*) and blue (*T. anthracinum*) color.

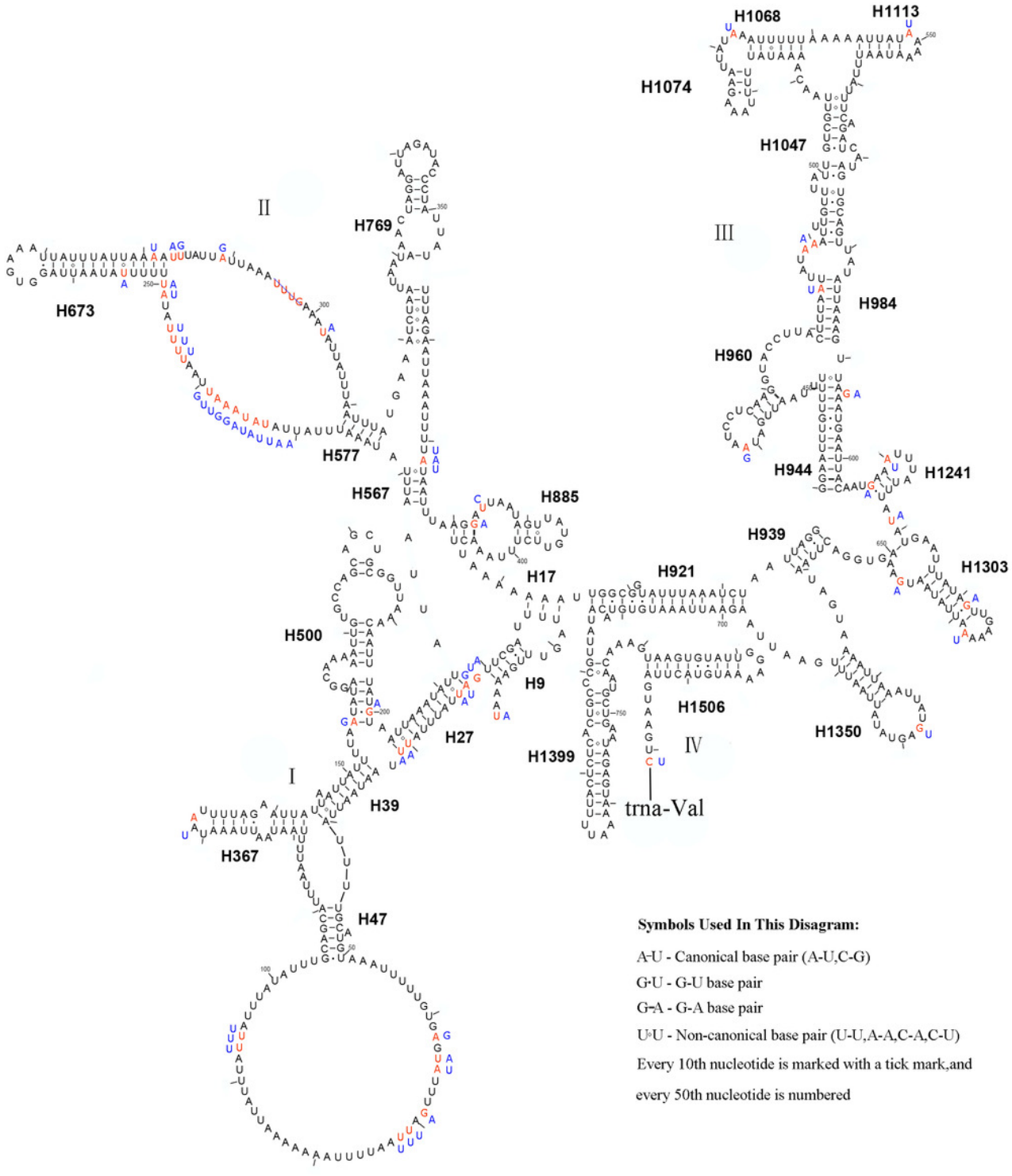
H1068
H1113
H1074
H1047
II
H769
III
H673
H984
H960
H577
H944
H1241
H567
H885
H939
H17
H921
H1303
H500
H9
H1506
H27
H1350
H1399
IV
I
H39
trna-Val
H367
H47
Symbols Used In This Disagram:
A-U - Canonical base pair (A-U,C-G)
G-U - G-U base pair
G-A - G-A base pair
U-U - Non-canonical base pair (U-U,A-A,C-A,C-U)
Every 10th nucleotide is marked with a tick mark,and
every 50th nucleotide is numbered

Figure 11

Corynis lateralis rrnS

Predicted *rrnS* secondary structure in *C. lateralis.* The numbering of helix follows Gillespie et al. (2006). Roman numbers refer to domain names.

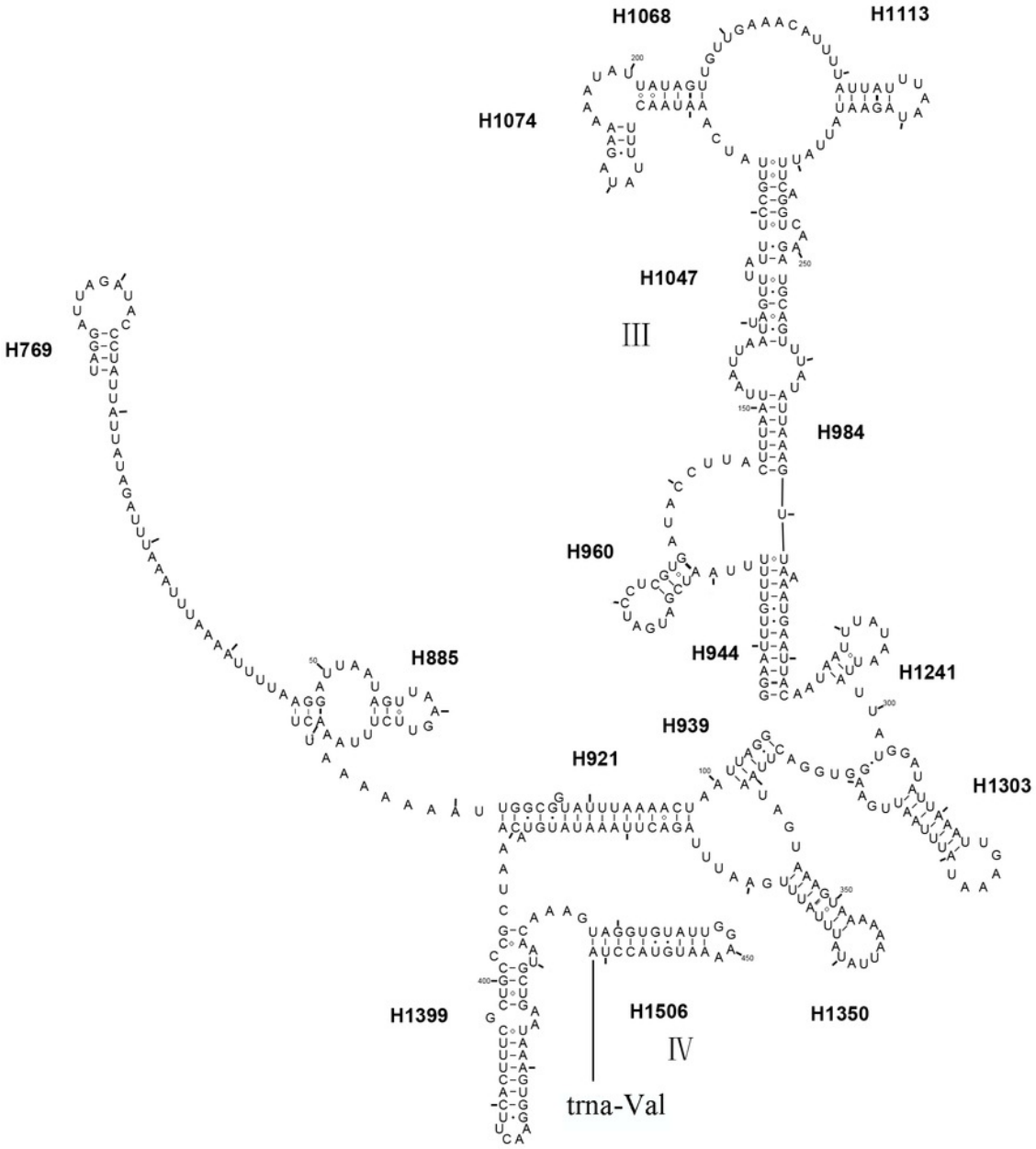

Symbols Used In This Disagram:

A-U - Canonical base pair (A-U,C-G)

G·U - G-U base pair

G-A - G-A base pair

U◦U - Non-canonical base pair (U-U,A-A,C-A,C-U)

Every 10th nucleotide is marked with a tick mark,and every 50th nucleotide is numbered

Figure 12

The phylogenetic tree of Symphyta from iqtree analysis.

Phylogenetic tree of Symphyta, based on ML analysis of the 13 PCGs (*ND2*, *COXI1*, *COX2*, *ATP8*, *ATP6*, *COX3*, *ND3*, *ND5*, *ND4*, *ND4L*, *ND6*, *CYT8*, and *ND1*) and 2 rRNAs (*rrnL* and *rrnS*) data set. Values branches represent maximum likelihood bootstrap clade frequency (CF) support. The scale bar indicates the number of substitutions per site.

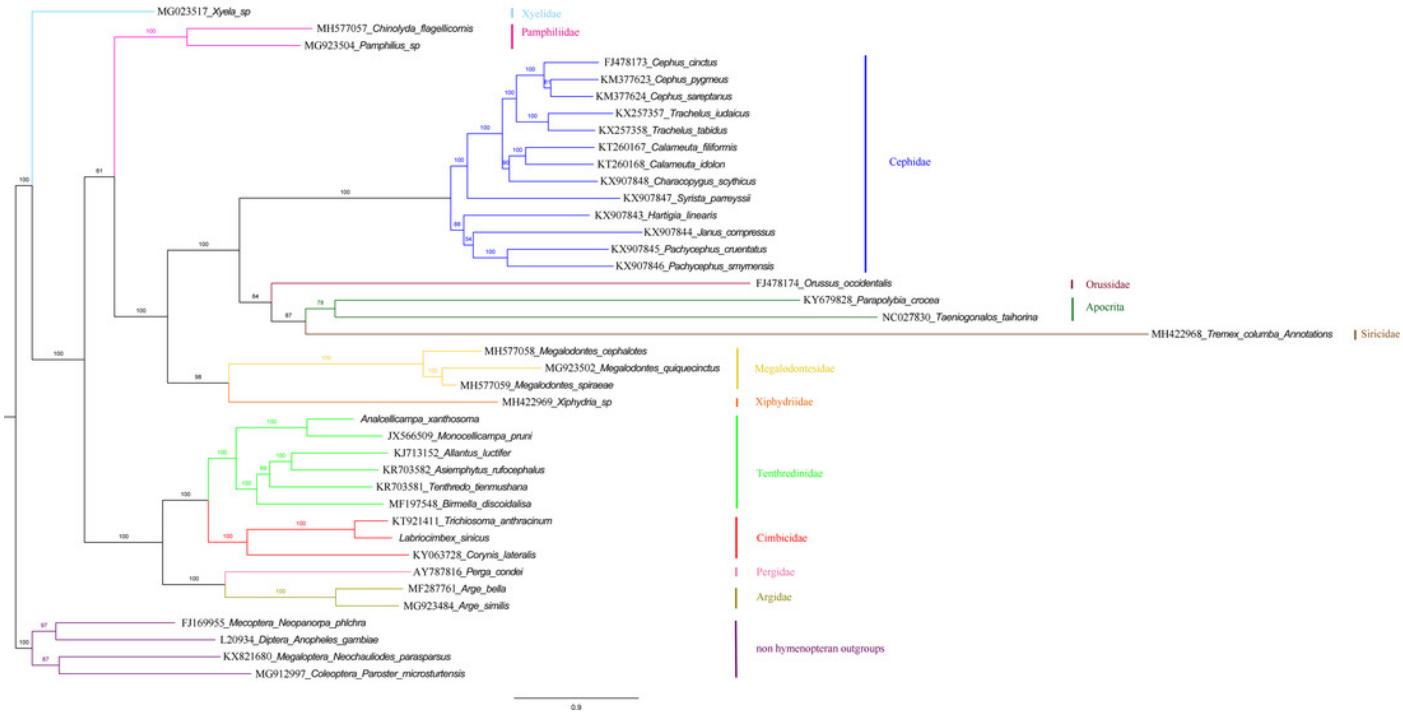

Figure 13

The phylogenetic tree of Symphyta from Bayesian analysis.

Phylogenetic tree of Symphyta, based on BI analysis of the 13 PCGs (*ND2*, *COXI1*, *COX2*, *ATP8*, *ATP6*, *COX3*, *ND3*, *ND5*, *ND4*, *ND4L*, *ND6*, *CYT8*, and *ND1*) and 2 rRNAs (*rrnL* and *rrnS*) data set. Values branches represent BI posterior probability (PP) support. The scale bar indicates the number of substitutions per site.